

Danno da radiazione in semiconduttori

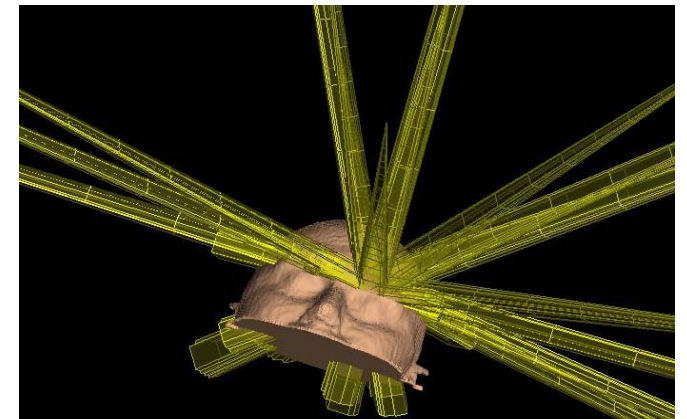
Mara Bruzzi

INFN, University of Florence, Italy

- ✓ Richiami sui dispositivi a semiconduttore:
 - ambienti operativi e livelli di irraggiamento
- ✓ Danno da radiazione microscopico
- ✓ Danno da radiazione macroscopico (Si)
- ✓ Material Engineering (Si)
- ✓ Cenni ai Materiali ad elevato bandgap
- ✓ Conclusioni

Ambienti operativi ove è richiesta resistenza al danno da radiazione

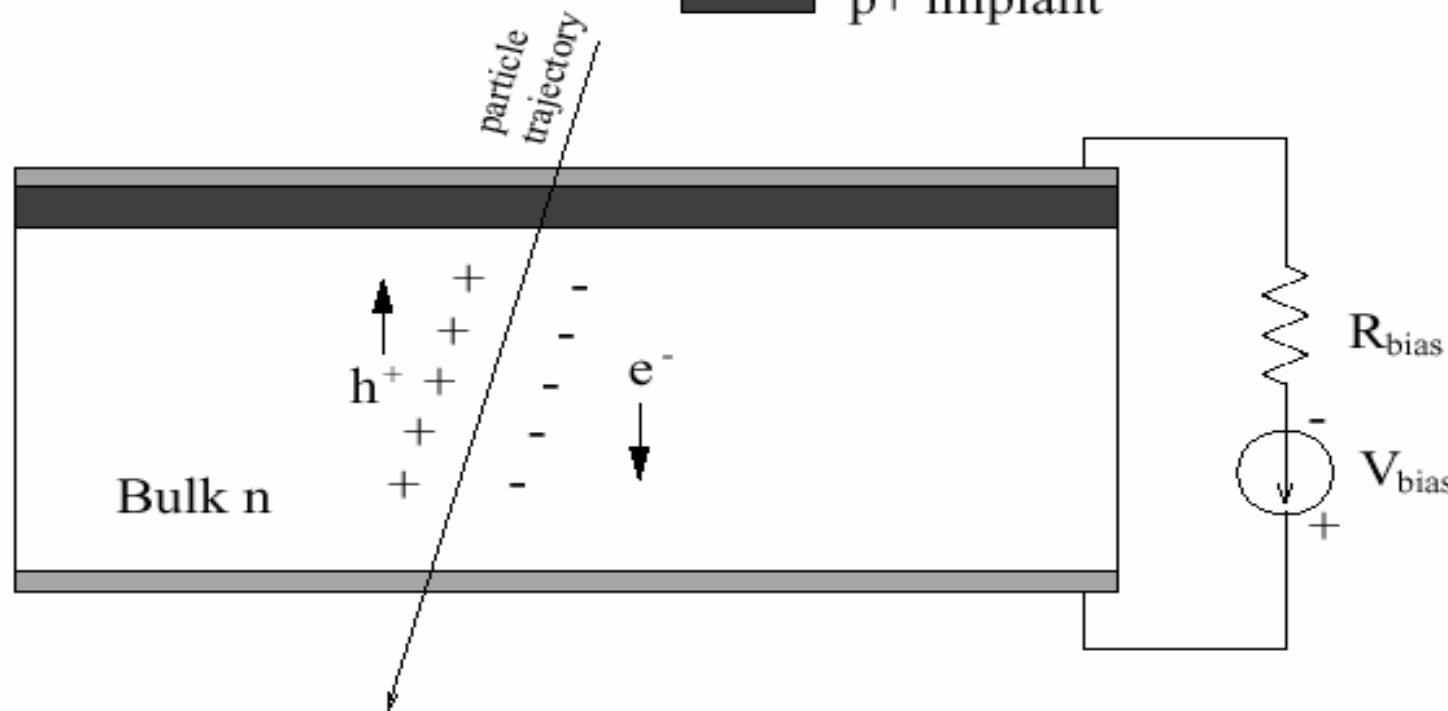
1. Rivelatori di posizione per esperimenti di alte energie
2. Celle solari in applicazioni spaziali
3. Dosimetri in radioterapia clinica



Principio di funzionamento di un rivelatore a semiconduttore

Giunzione p⁺n

metal
p⁺ implant



Contatto ohmico

Isolante $\rho > 10^{10} \Omega \text{cm}$

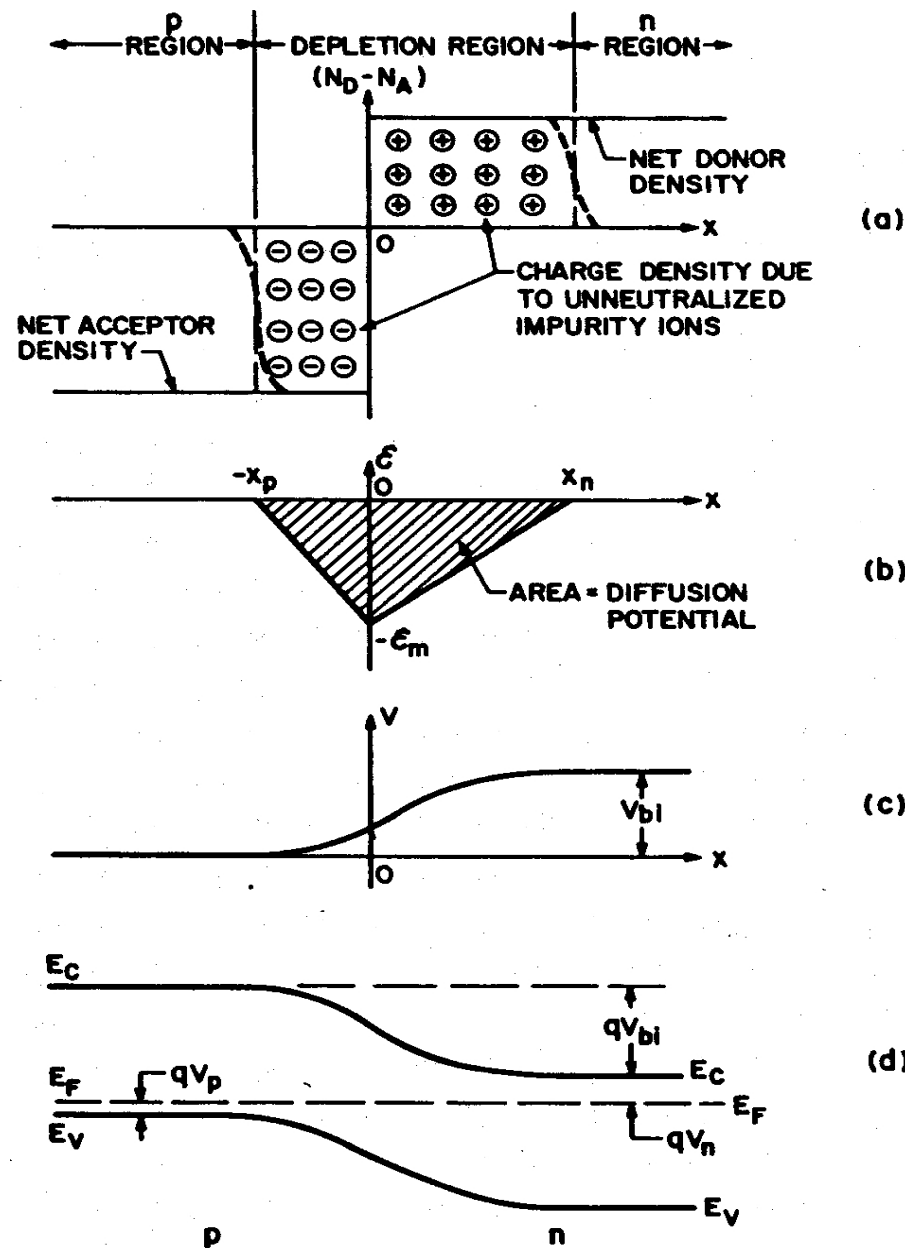
Contatto ohmico

Contatto Schottky

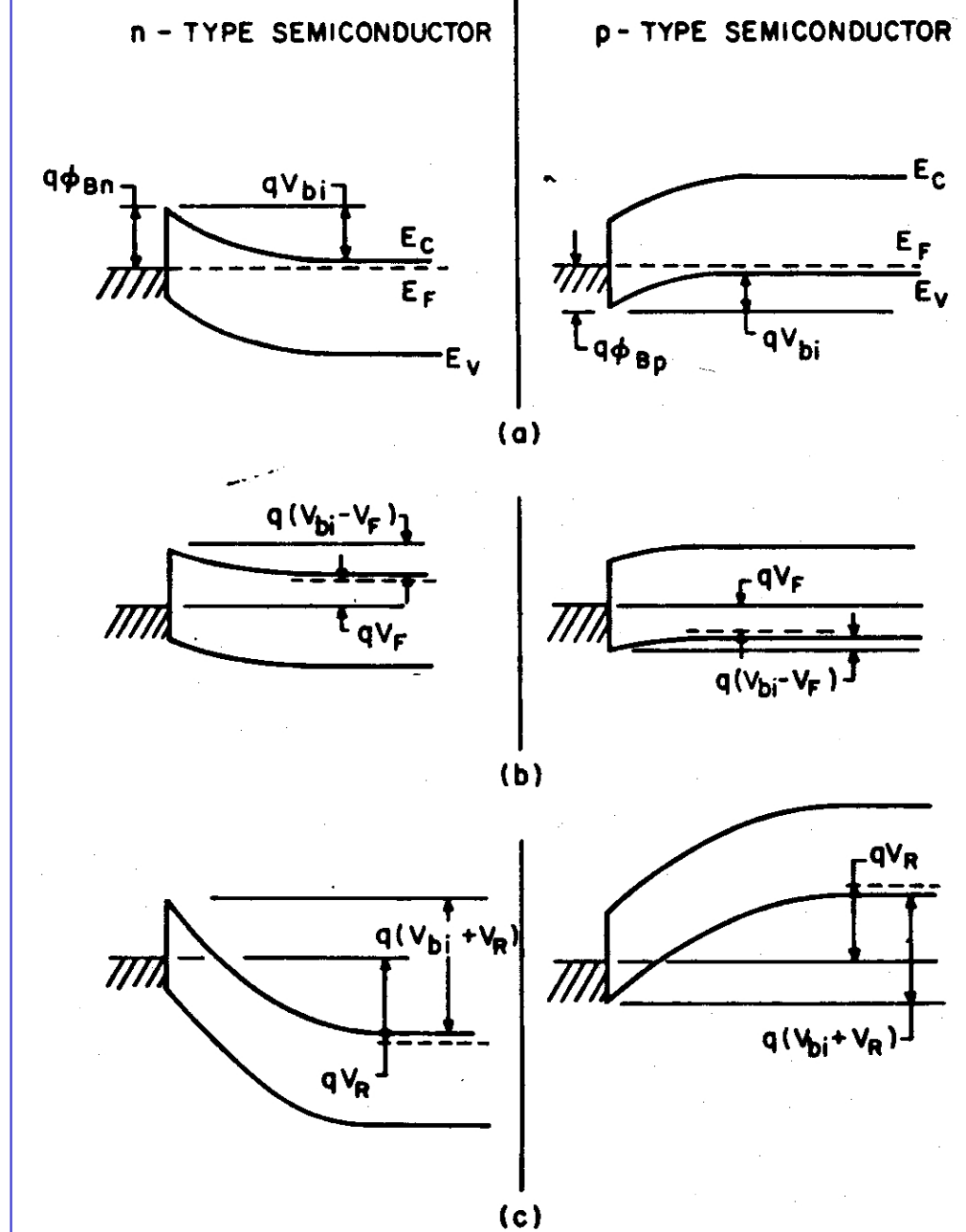
Semiconduttore tipo n o p

Contatto ohmico

Giunzione p-n



Giunzione Schottky



Grandezze fisiche di rilievo per la giunzione Schottky o p-n

Corrente di fuga

$$J_{inversa} = \frac{1}{2} q \frac{n_i}{\tau_0} W \alpha \sqrt{V_{rev}}$$

Corrente diretta

$$J_{diretta} \propto e^{qV/nKT}$$

Capacità

$$C = \frac{\epsilon \cdot Area}{d}$$

Spessore della regione attiva

$$d = \sqrt{\frac{2\epsilon}{qN_{eff}} (V_{rev} + V_{built-in}) + L_{diff}}$$

**Concentrazione di carica fissa
nella regione svuotata**

$$N_{eff} = \frac{2 \cdot \epsilon \cdot (V_{dep} + V_{bi})}{q \cdot W^2}$$

Resistività

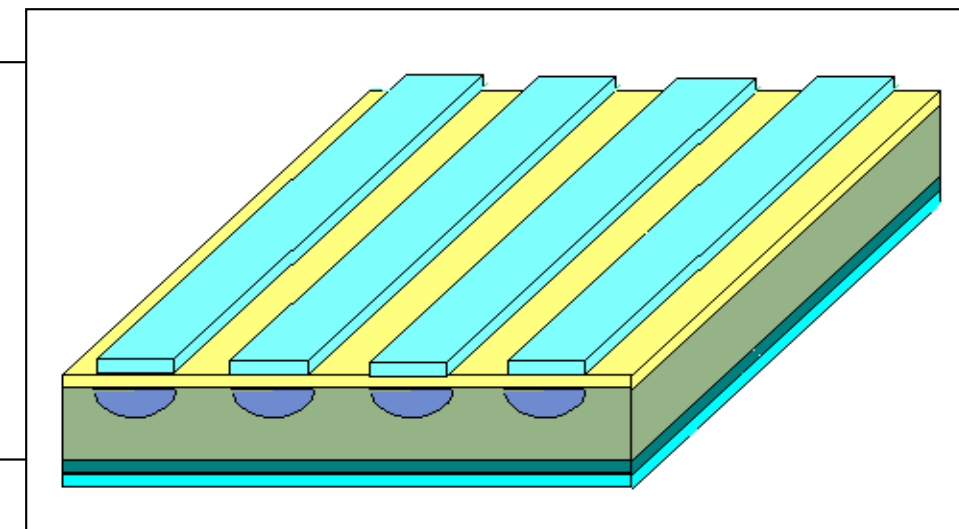
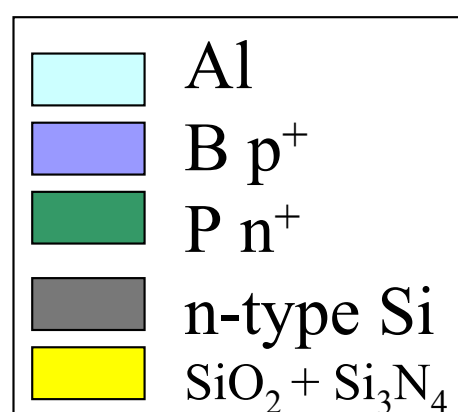
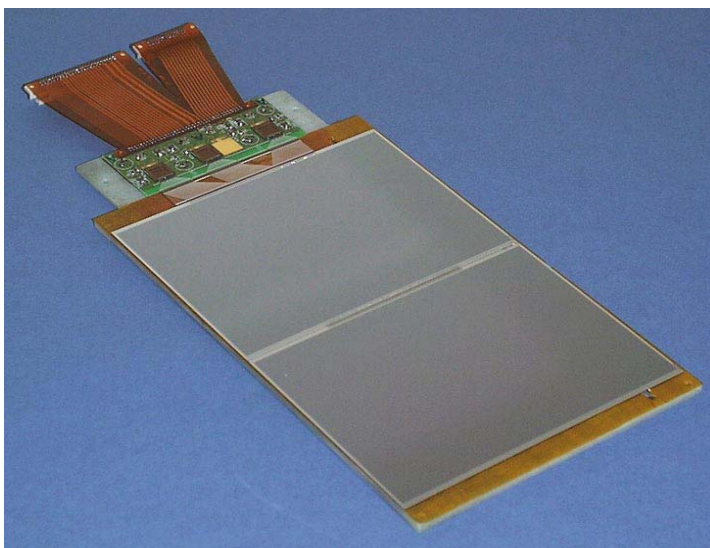
$$\rho = \frac{1}{q \cdot \mu \cdot N_{eff}}$$

1. Rivelatore di posizione per esperimenti di fisica delle alte energie

Float Zone Silicon $\rho = 1-6 \text{ k}\Omega\text{cm}$

Orientazione $<111>$, $<100>$

thickness $\sim 300\mu\text{m}$ module length $\approx 10\text{cm}$ strip width $w \approx 15 \mu\text{m}$, pitch $p \approx 50-200\mu\text{m}$.



Ambiente operativo e livelli di irraggiamento

High energy Physics experiments at Large Hadron Collider (LHC), CERN, Geneva

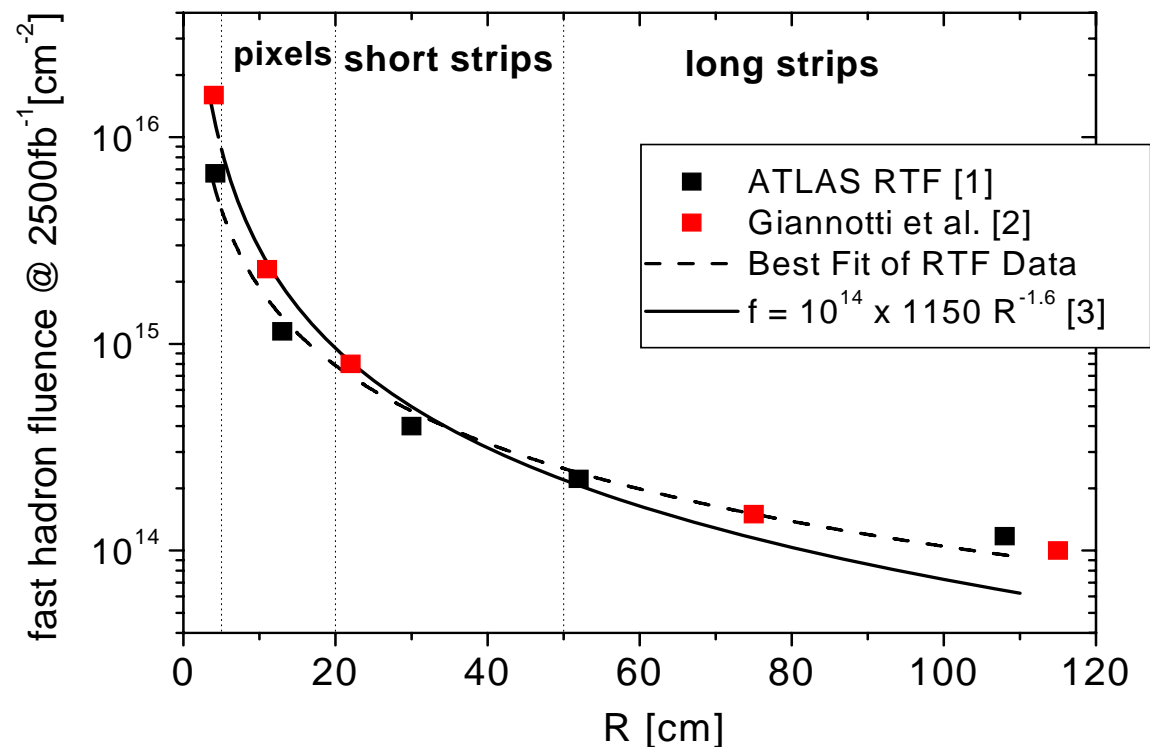
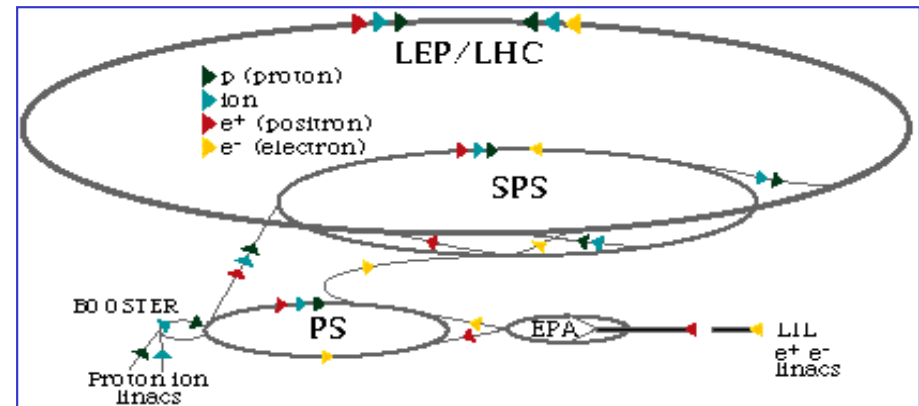
p-p collision $L \sim 10^{34} \text{ cm}^{-2} \text{ s}^{-1}$

$E_{\text{cm}} = 14 \text{ TeV}$

Increase of luminosity of LHC up to $10^{35} \text{ cm}^{-2} \text{ s}^{-1}$ discussed since 2002. Date for upgrade ~ 2015 .

Main constraint is the survival of the Si detector tracker to the exceptionally high fluences of fast hadrons.

See next talk by M. Moll

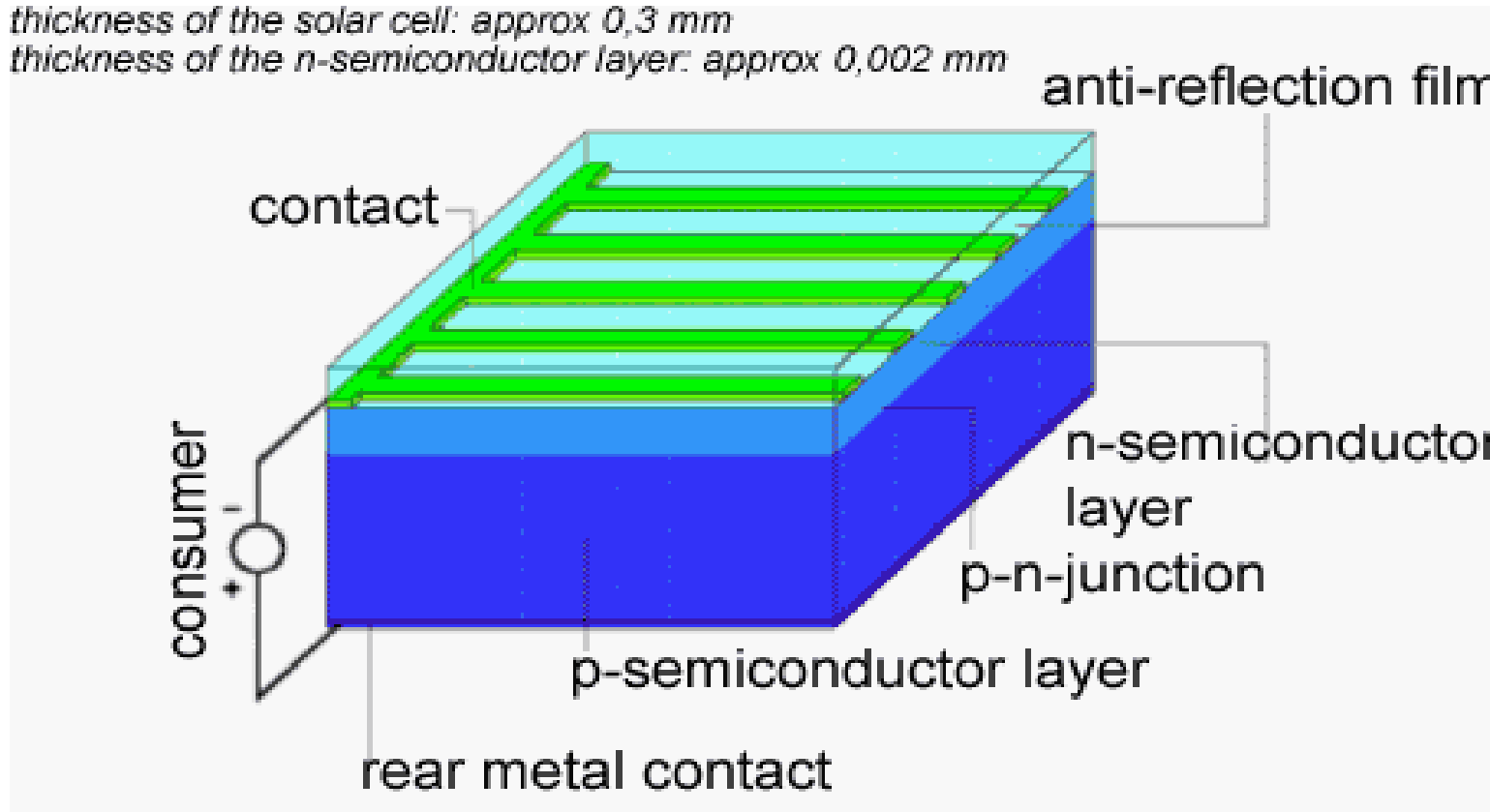


Solar cells

Typical solar cell module is composed of n⁺/p/p⁺ junctions made on Silicon, used in photovoltaic mode. The built-in electric field leads to the separation of the charge carriers that are released by light. Silicon cells are approximately 10 cm by 10 cm large (recently also 15 cm by 15 cm). A transparent anti-reflection film protects the cell and decreases reflective loss on the cell surface.

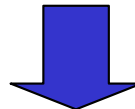
thickness of the solar cell: approx 0,3 mm

thickness of the n-semiconductor layer: approx 0,002 mm



Caratteristiche importanti in un rivelatore di radiazione

- Elevato segnale / sensibilità (corrente / carica)
- Basso rumore
- minimo ingombro spaziale / massimo volume attivo
- Elevata velocità di risposta: $v = \mu E$
- Stabilità con la dose accumulata



- ● Bassa energia per creazione coppia e-h → gap piccolo
- ● Bassa corrente di buio → gap elevato
- ● Bassa tensione di completo svuotamento
- ● Elevata mobilità'
- ● Elevata resistenza al danno da radiazione

Solar cell efficiency factors

Maximum-power point

By increasing the resistive load on an irradiated cell continuously from zero (a *short circuit*) to a very high value (an *open circuit*) one can determine the maximum-power point, that is, the load for which the cell can deliver **maximum electrical power** at that level of irradiation. $V_m \times I_m = P_m$.

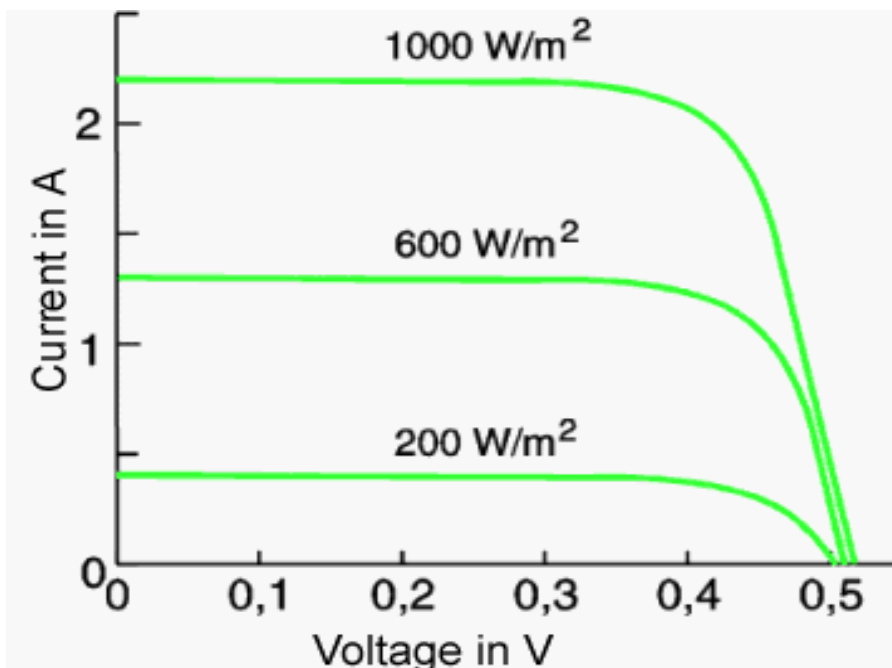
Energy conversion efficiency

A solar cell's *energy conversion efficiency* (η), is the percentage of power converted from absorbed light to electrical energy, calculated as P_m divided by the input light *irradiance* under "standard" test conditions (E , in W/m^2) and the *surface area* of the solar cell (A_c in m^2).

$$\eta = \frac{P_m}{E \times A_c}$$

Fill factor

Another defining term in the overall behavior of a solar cell is the *fill factor* (FF). This is the ratio of the **maximum power divided by the open circuit voltage (V_{oc}) and the short circuit current (I_{sc})**:



$$FF = \frac{P_m}{V_{oc} \times I_{sc}} = \frac{\eta \times A_c \times E}{V_{oc} \times I_{sc}}$$

Ambiente operativo e livelli di irraggiamento

Main sources of radiation affecting PV modules are **protons and electrons trapped by the terrestrial magnetic field and protons coming from the Sun**, the particle flux depending on the orbit of the mission. Radiation damage in satellites at low altitude orbits (lower than 800 km) or in the high altitude ones (5000 km or higher) is mainly produced by protons (close to 90% of damage).

Most advantageous orbits for a global satellite network, both from cost and operational viewpoints, may be in Medium Earth Orbits (MEO), in the 2000–10 000 km range. Unfortunately, these orbits are in the midst of the Van Allen radiation belts, where the severe radiation environment causes a rapid degradation of the solar cells.

Semiconductor Devices in Clinical Radiotherapy

Silicon diodes are commonly used for *in-vivo* dosimetry and other radiotherapy applications such as dosimetric verification of stereotactic beams. With respect to ionization chambers they are characterized by faster responses and higher sensitivities, this latter property allow them to be produced with significantly smaller dimensions. They are usually made on p type Czochralski or n-type FZ Si 300-500 μ m thick wafers, 10 Ω cm. They work in PV mode to minimize the leakage current. Typical irradiation: γ -rays from Co⁶⁰, 6-25MeV e (lifetime up to 1-10kGy) and 10-200MeV protons.



MapCHECK (Sun Nuclear Corp.) Matrix
of Si p-n junction for pre-treatment
verification in clinical radiotherapy

**Acceleratore lineare e⁻ 6-25 MeV
Ospedale Careggi - Firenze**



Regione attiva in un dosimetro per radioterapia

La sensibilità del dosimetro è direttamente proporzionale alla larghezza della regione attiva: $s \propto W_D$. Il dispositivo lavora con $V_{bias} = 0$.

$$W_D = W_0 + L = \sqrt{\left(\frac{2 \cdot \varepsilon \cdot V_{bi}}{q \cdot N_{eff}} \right)} + \sqrt{D_h \cdot \tau_h}$$

Lunghezza di diffusione per i portatori minoritari

$$D_h = \mu_h K \cdot T / e$$

τ_h = tempo di vita media del portatore minoritario

Danno da radiazione nei materiali semiconduttori

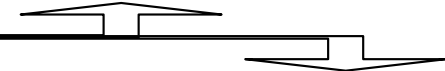
Danno microscopico

- Creazione di difetti

Trappole

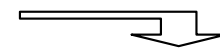


Centri di ricombinazione



difetti estesi o clusters

- Rimozione / compensazione dei difetti superficiali



Pinning del livello di Fermi a centro gap

Danno macroscopico

- Aumento della corrente di buio
- Variazione di N_{eff} e del tipo di spazio di carica - aumento della resistività
- diminuzione del tempo di vita medio dei portatori minoritari

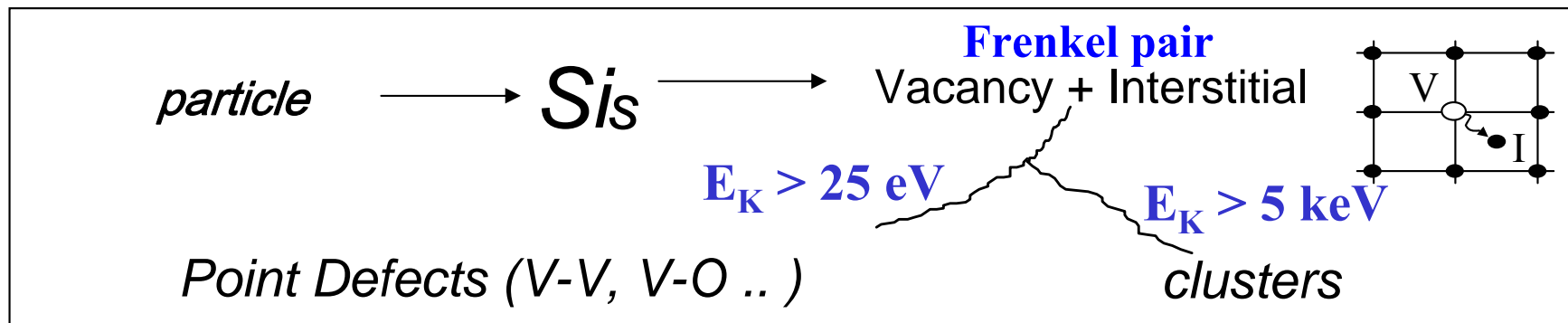
Diminuzione della efficienza di raccolta di carica



Diminuzione della lunghezza di diffusione per minoritari

Danno da radiazione microscopico

Creation of Radiation Induced lattice defects



Simulation of Microscopic Damage

- ✓ Generation of hadronic interactions
- ✓ Transport of the produced heavy recoils
- ✓ Migration of V and I to form stable defects

[Mika Huhtinen NIMA 491(2002) 194]

Vacancy amount and distribution depends on particle kind and energy

^{60}Co -gammas

- Compton Electrons with max. $E_\gamma \approx 1 \text{ MeV}$ (no cluster production)

Electrons

- $E_e > 255 \text{ keV}$ for displacement
- $E_e > 8 \text{ MeV}$ for cluster

Neutrons (elastic scattering)

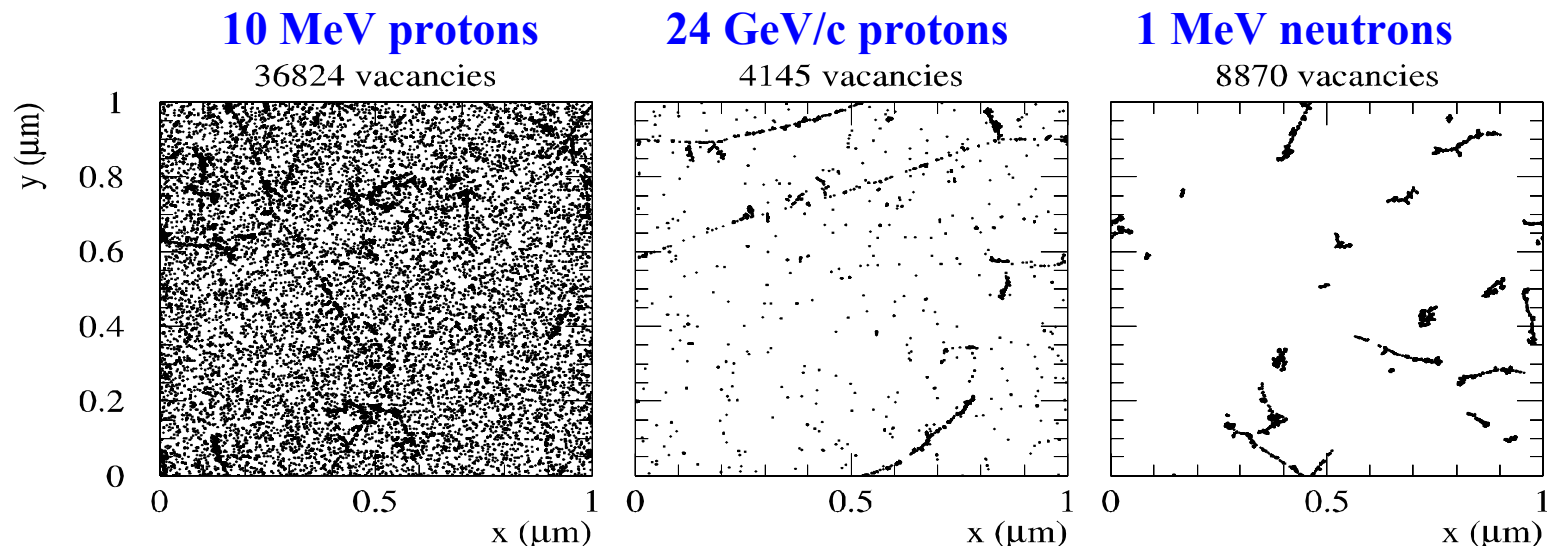
- $E_n > 185 \text{ eV}$ for displacement
- $E_n > 35 \text{ keV}$ for cluster

Only point defects

↔ point defects & clusters

↔ Mainly clusters

Initial distribution of vacancies in $(1\mu\text{m})^3$ after 10^{14} particles/cm²



[Mika Huhtinen NIMA 491(2002) 194]

Primary Damage and secondary defect formation

- Two basic defects

I - Silicon Interstitial V - Vacancy

- Primary defect generation

I, I_2 higher order I (?)

$\Rightarrow I$ - CLUSTER (?) ←

V, V_2 , higher order V (?)

$\Rightarrow V$ - CLUSTER (?) ←

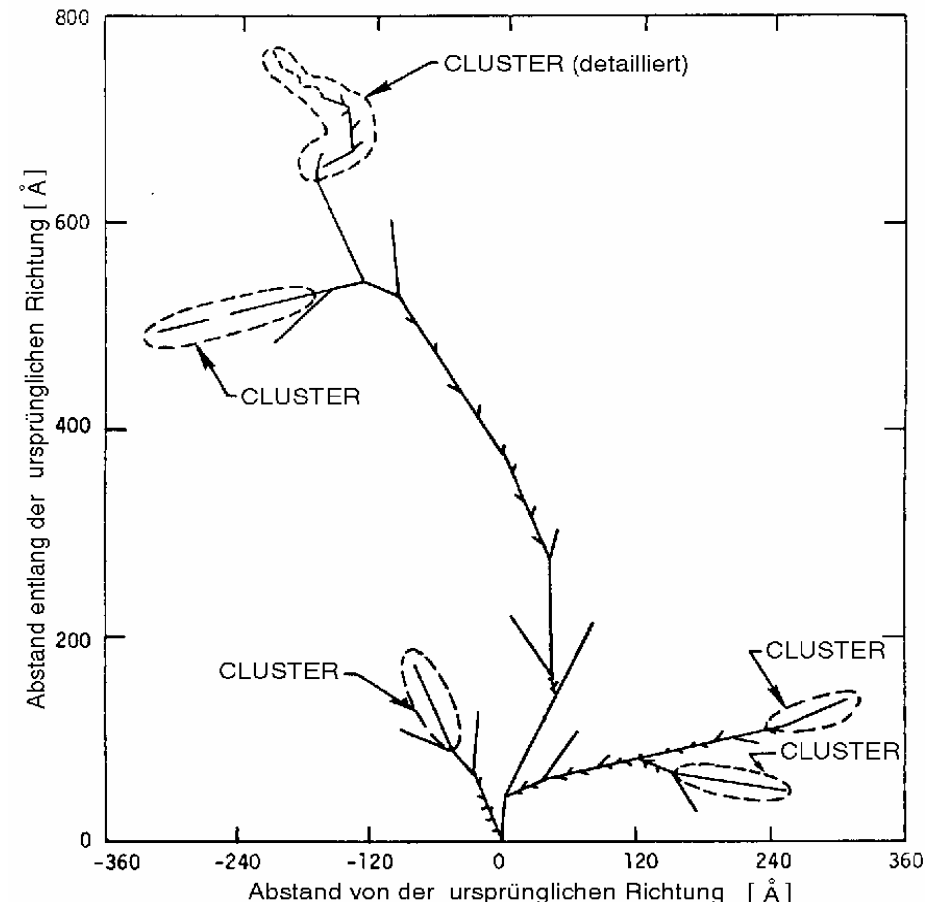
- Secondary defect generation

Dopants : P, B

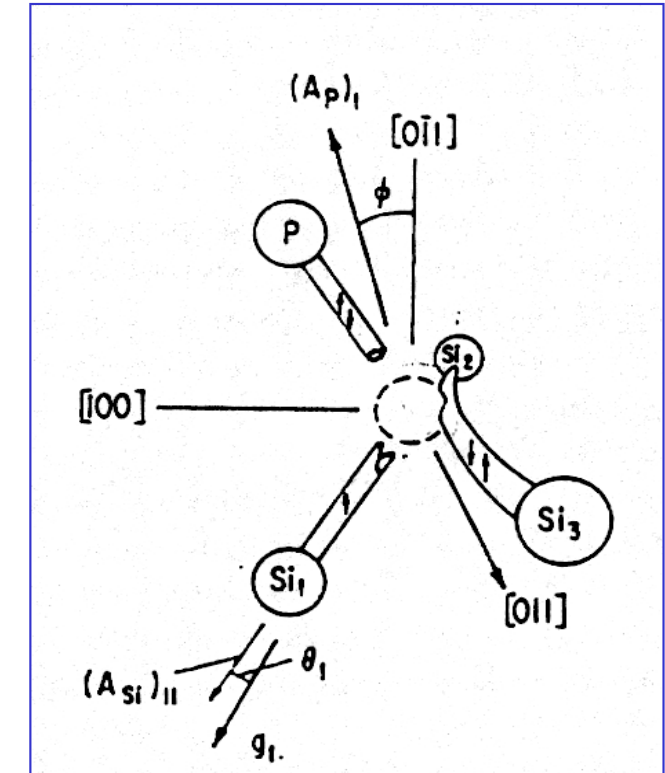
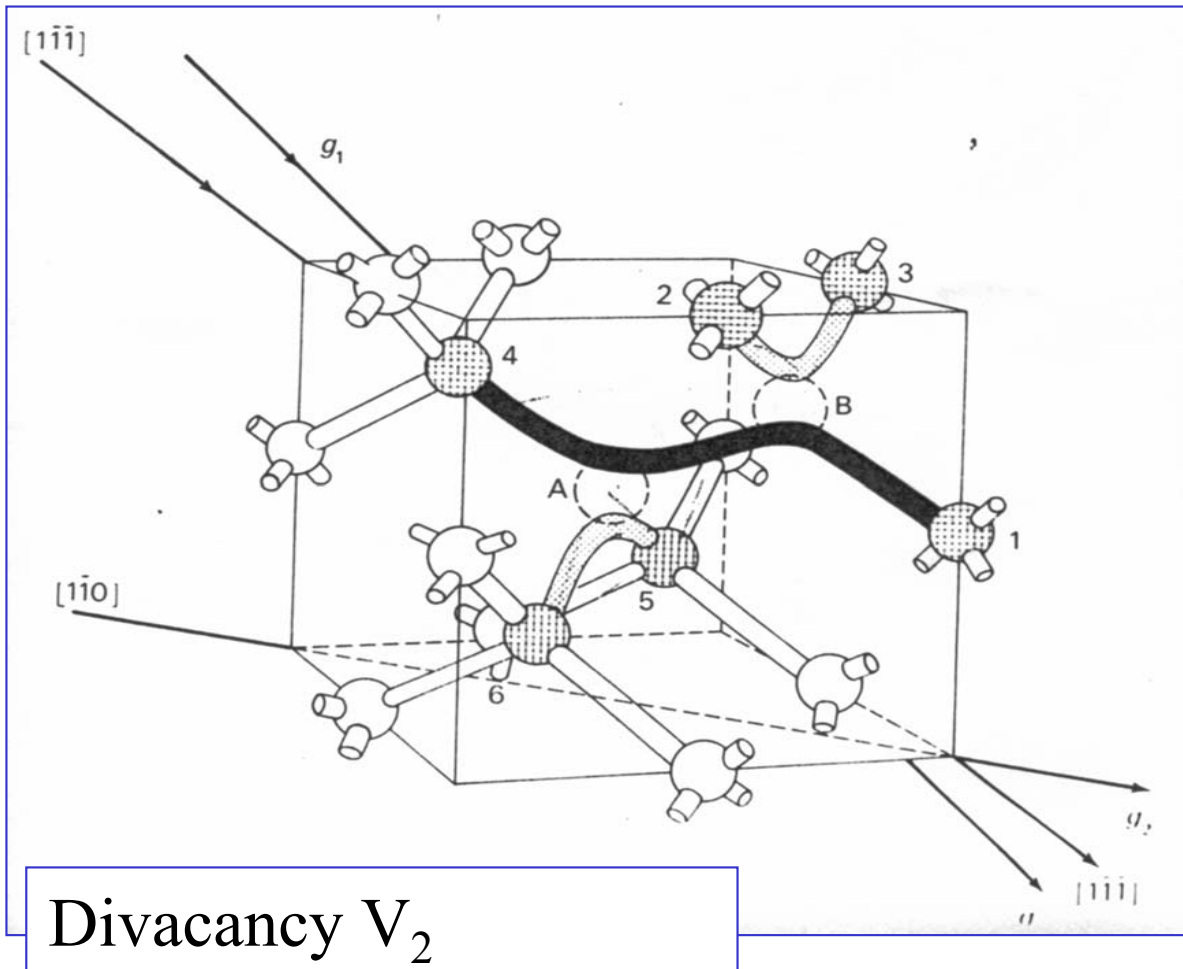
Main impurities in silicon: Carbon C_s

Oxygen O_i

Oxygen dimer: O_{2i}



Radiation Induced defects related to the lattice vacancy

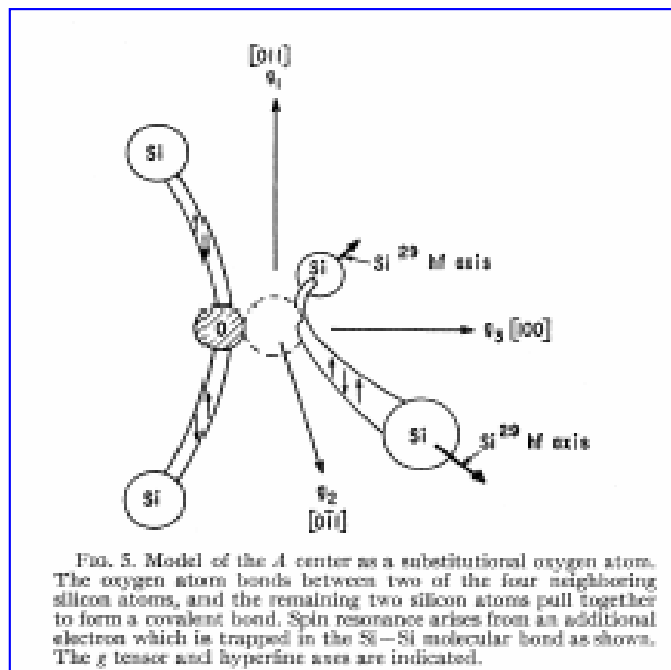


Phosphorous-Vacancy
P-V (E centre)

Corbett, Watkins et al, PRB, 60s

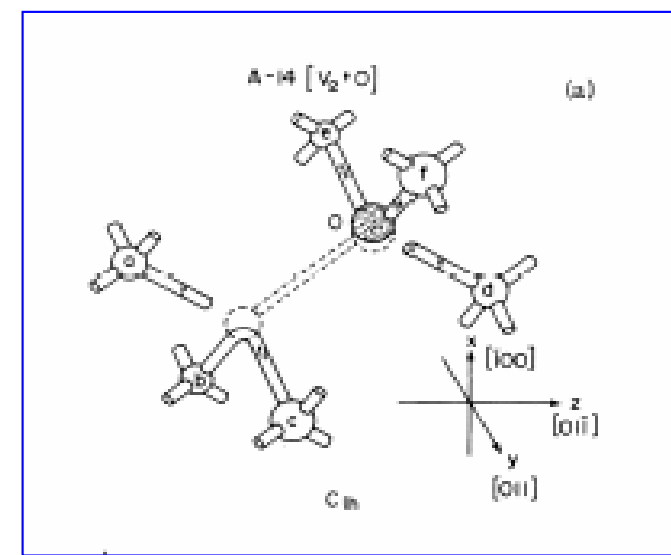
Radiation Induced Defects related to Oxygen

FZ Si [O_i] $\sim 10^{15}$ cm⁻³ ; CZ Si [O_i] $\sim 10^{18}$ cm⁻³



V-O defect (A centre)

Watkins, Corbett: Phys.Rev.,121,4, (1961),1001



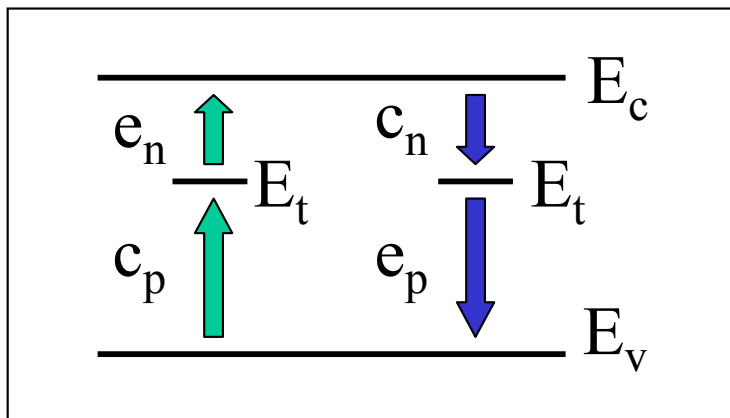
V₂O defect

Lee, Corbett: Phys.Rev.B,13,6, (1976),2653

Tecniche per l'analisi dei difetti in materiali semiconduttori

- 1. Thermally Stimulated Currents TSC**
- 2. Deep Level Transient Spectroscopy DLTS**
- 3. Photo Induced Current Transient Spectroscopy PICTS**

Energy Levels related to traps



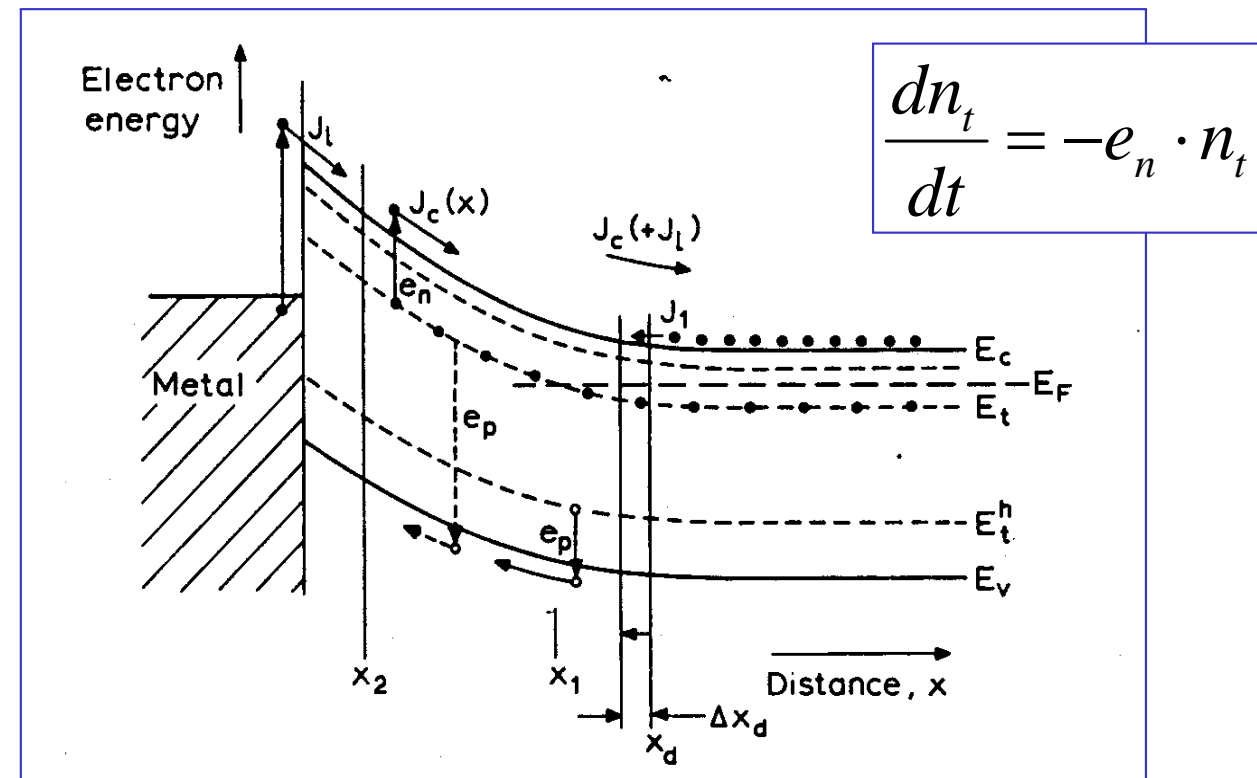
E_t, σ, N_t Trap parameters
 Concentration
 Cross section
 Activation energy

Emission coefficient:

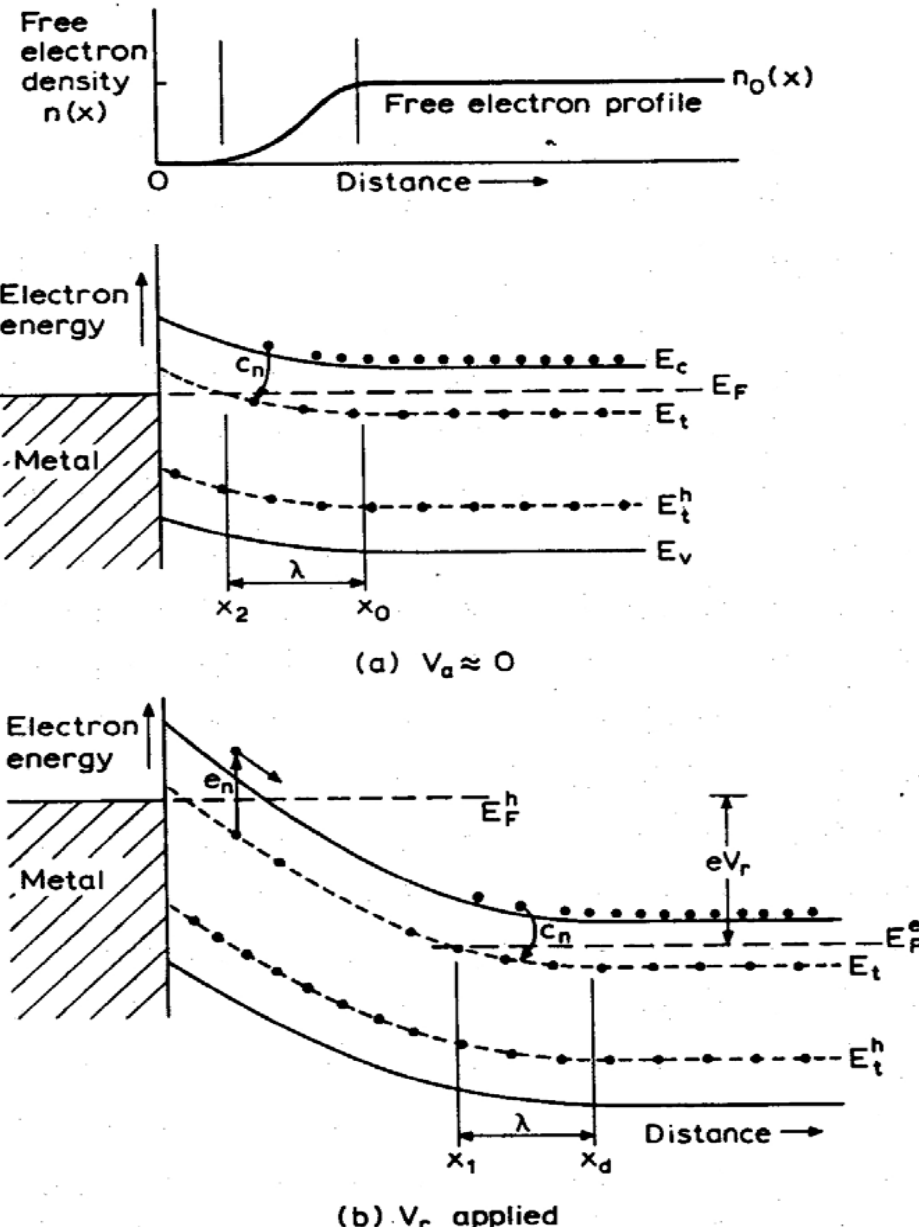
$$e_n = N_c \sigma_n v_{th} \cdot e^{-\frac{E_c - E_t}{KT}}$$

Capture coefficient :

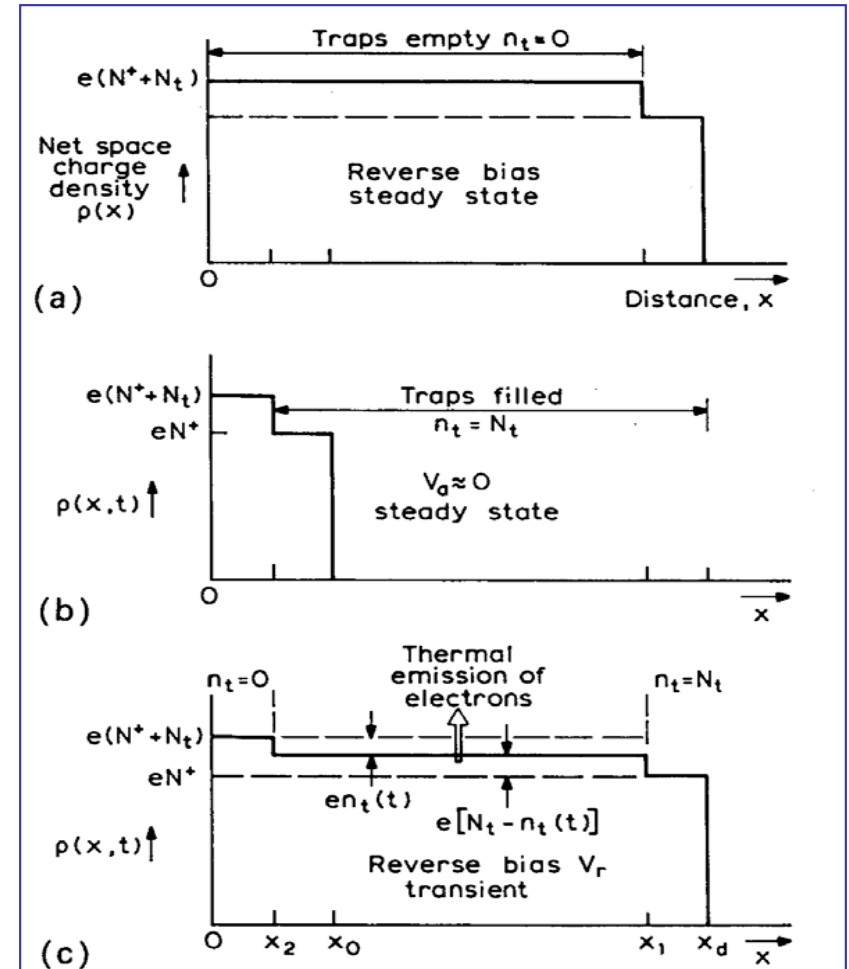
$$c_n = n \sigma_n v_{th}$$



Livelli energetici profondi in regione svuotata

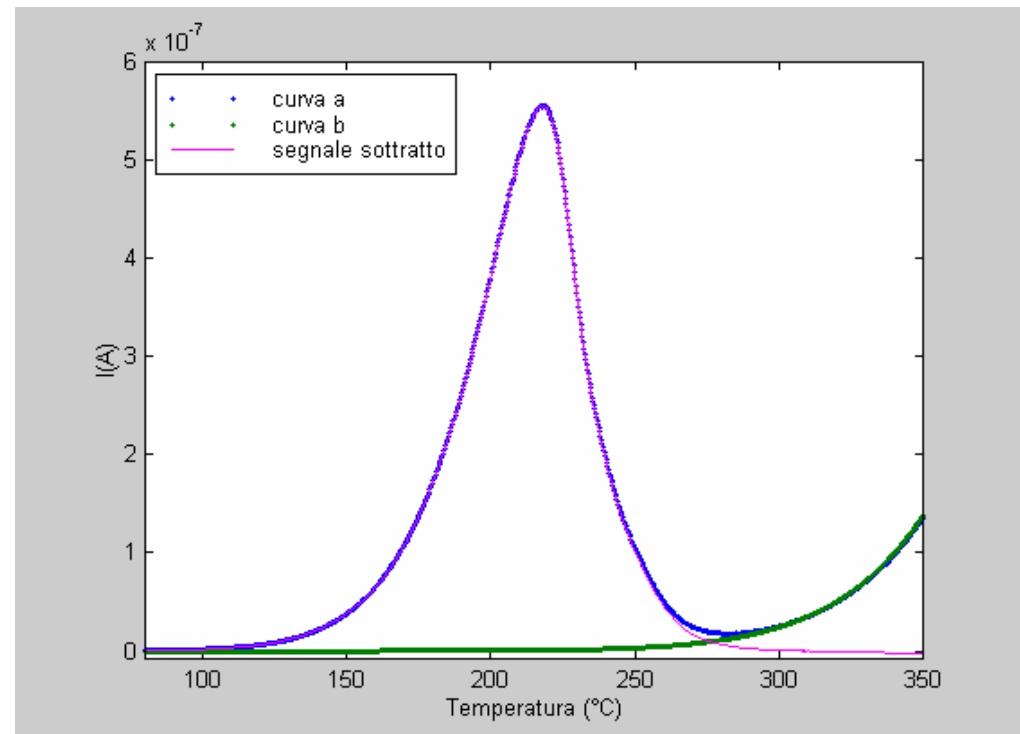
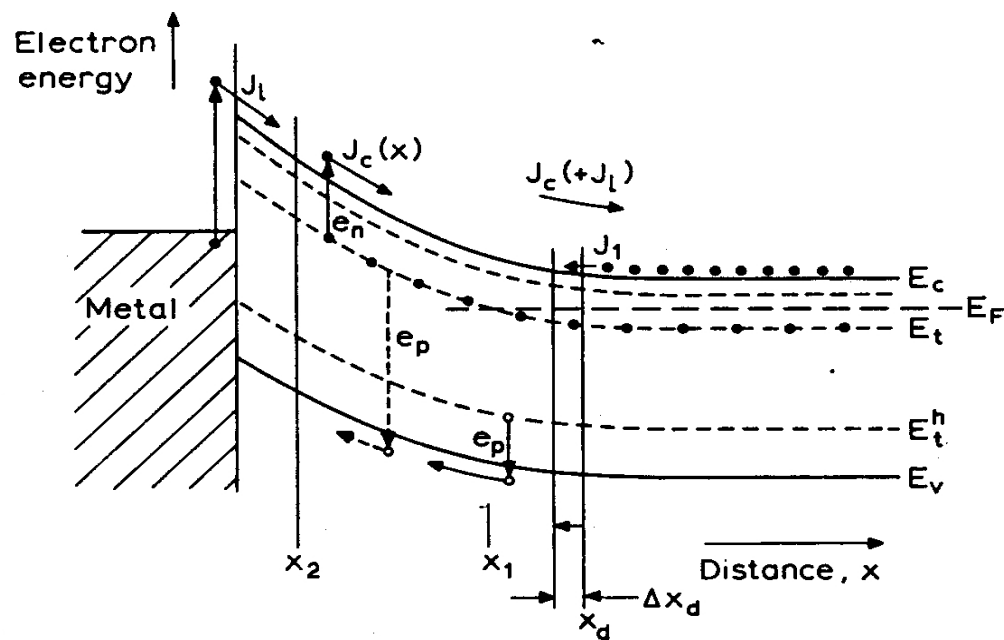


$$\frac{dn_t}{dt} = -e_n \cdot n_t$$



Thermally Stimulated Current TSC

$$J_{TSC} = J_c + \frac{\partial D}{\partial t} = -\frac{1}{2} q W_d e_n n_t$$

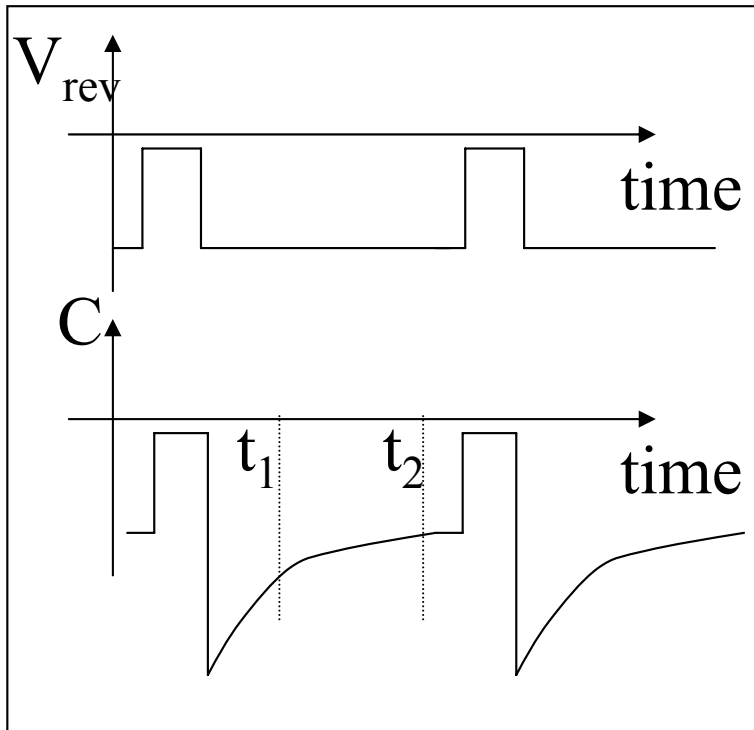


$$I_{TSC}(T) = -\frac{1}{2} q \cdot A \cdot N_t \cdot W \cdot e_n(T) \exp\left(-\frac{1}{b} \int_{T_i}^T e_n(T) dT\right)$$

Mara Bruzzi, Danno da radiazione in semiconduttori

Scuola Nazionale rivelatori ed elettronica per fisica delle alte energie , astrofisica 21 Aprile 2009, Legnaro, Italy

Deep Level Transient Spectroscopy DLTS



$$S = \Delta C_0 \left(e^{-e_n(T)t_1} - e^{-e_n(T)t_2} \right)$$

$$e_n(T_{\max}) = \frac{t_2 - t_1}{\ln(t_2/t_1)} \alpha T_{\max}^2 \cdot e^{-E_t / KT_{\max}}$$

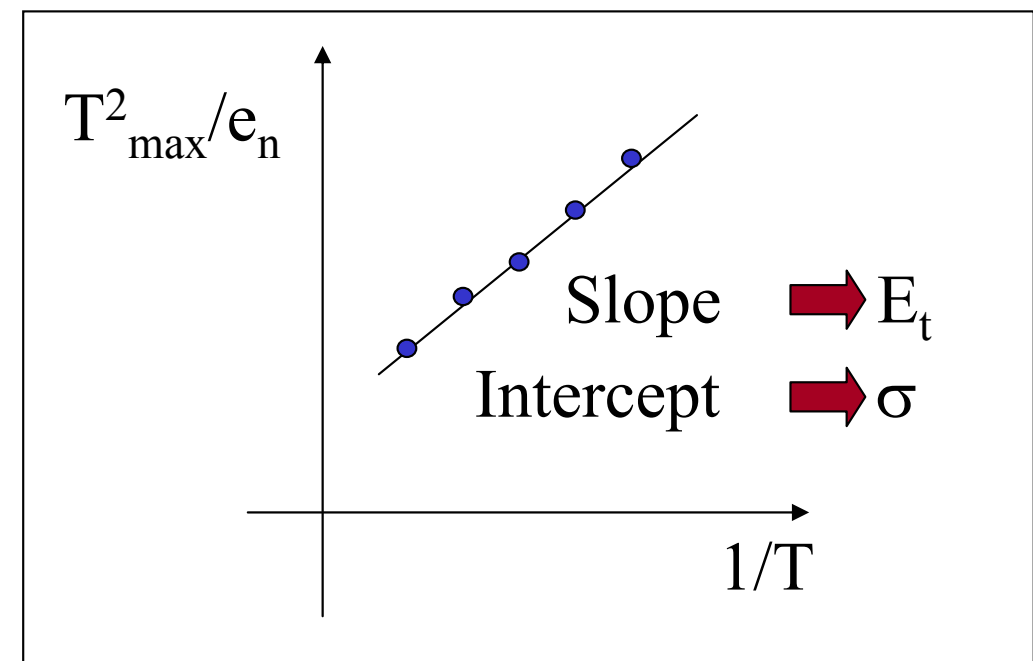
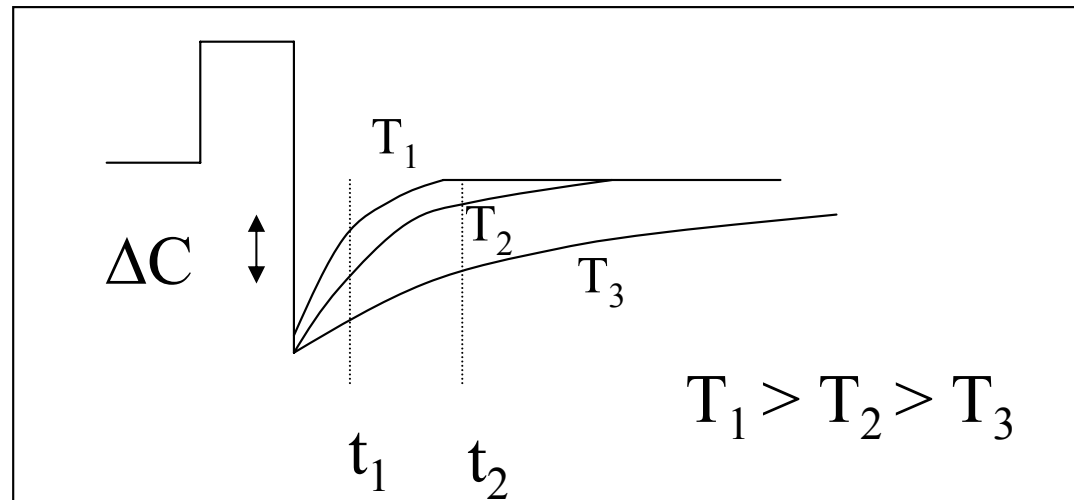
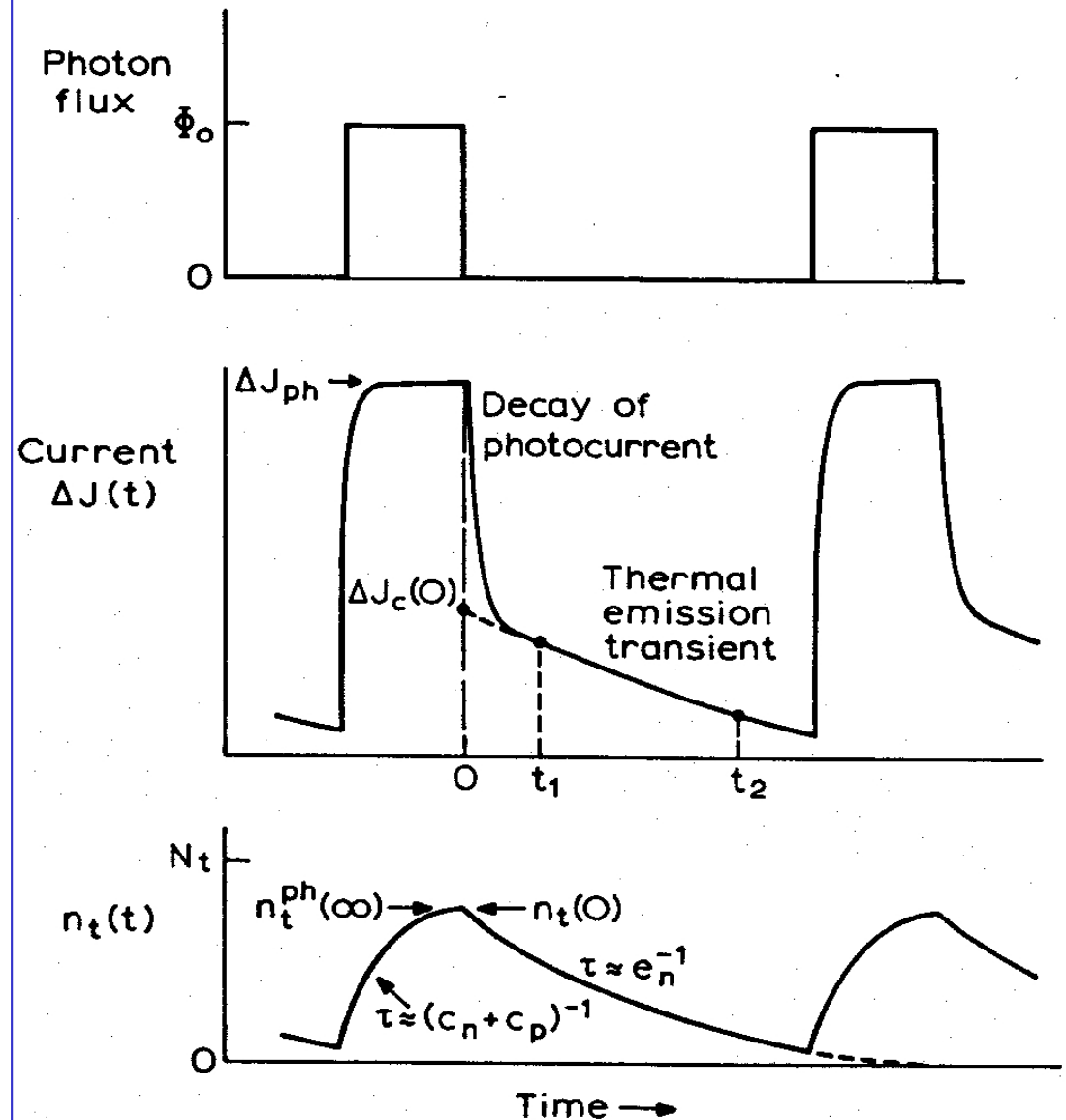
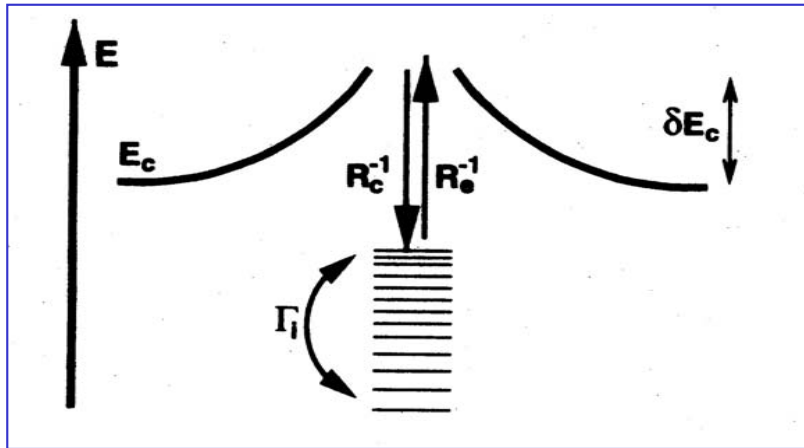


Photo Induced Current Transient Spectroscopy PICTS



Simile alla DLTS,
l'eccitazione delle trappole
viene effettuata mediante un
flusso di fotoni con $h\nu > E_g$ e
viene misurato il transiente in
corrente

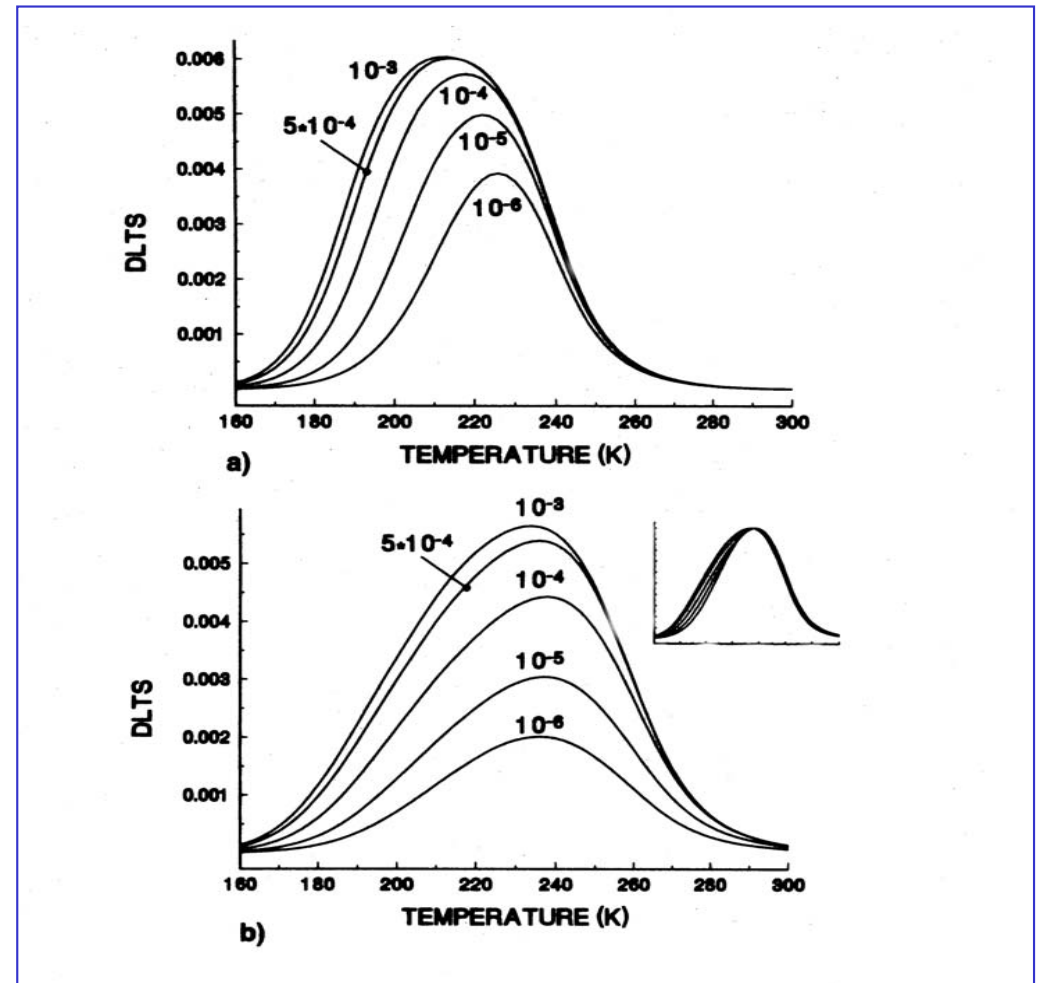
Visualizzazione dei clusters (difetti estesi) con tecniche DLTS



$$R_c(E, t) = \sigma_n v_{th} n [1 - f(E, t)] \exp\left[-\frac{\delta E_c}{kT}\right]$$

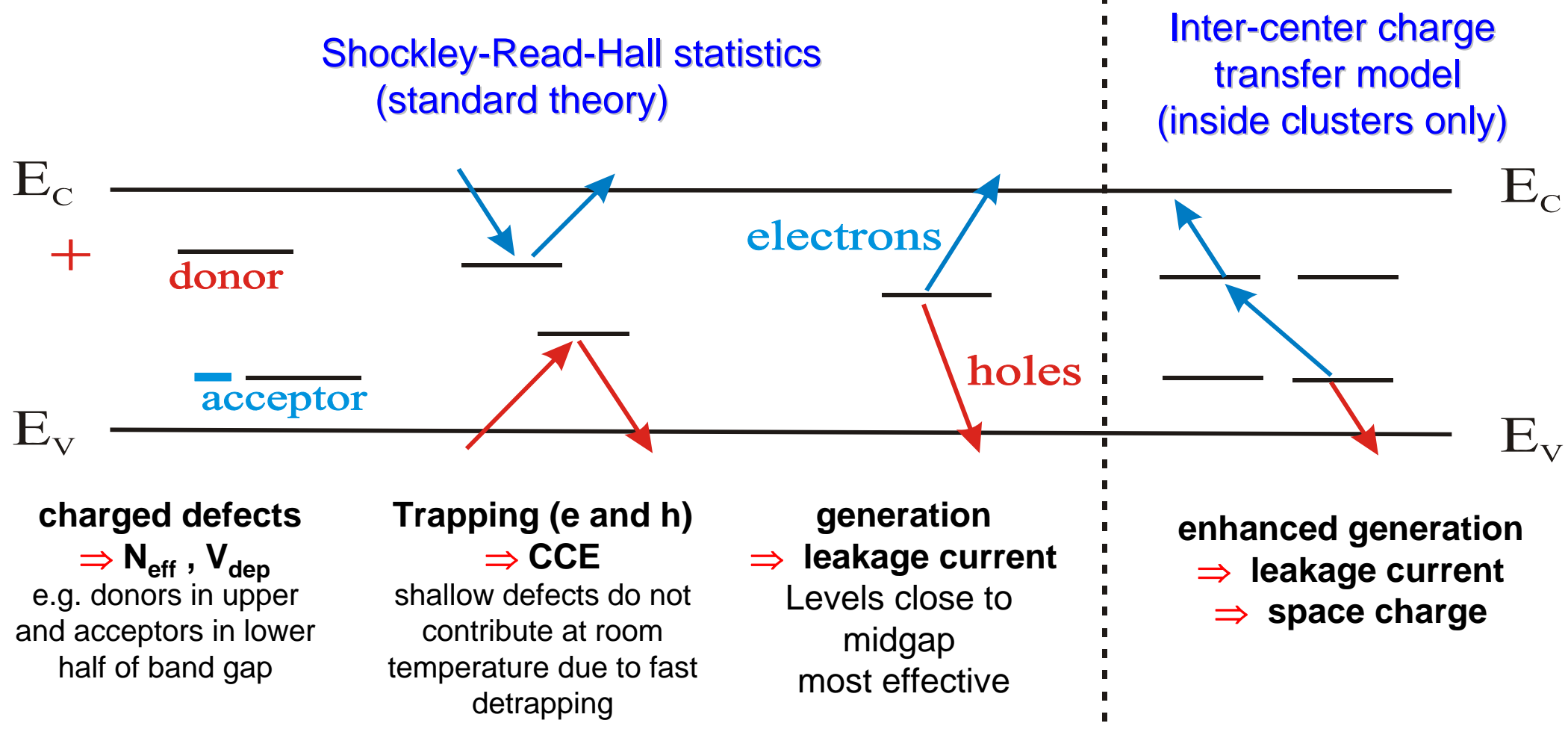
L'effetto è quello di un
allargamento del segnale DLTS

Una barriera di potenziale scherma il difetto esteso
alterando il segnale DLTS



Danno da radiazione macroscopico

Impact of Defects on Detector properties



Impact on detector properties can be calculated if all defect parameters are known:

$\sigma_{n,p}$: cross sections

ΔE : ionization energy

N_t : concentration

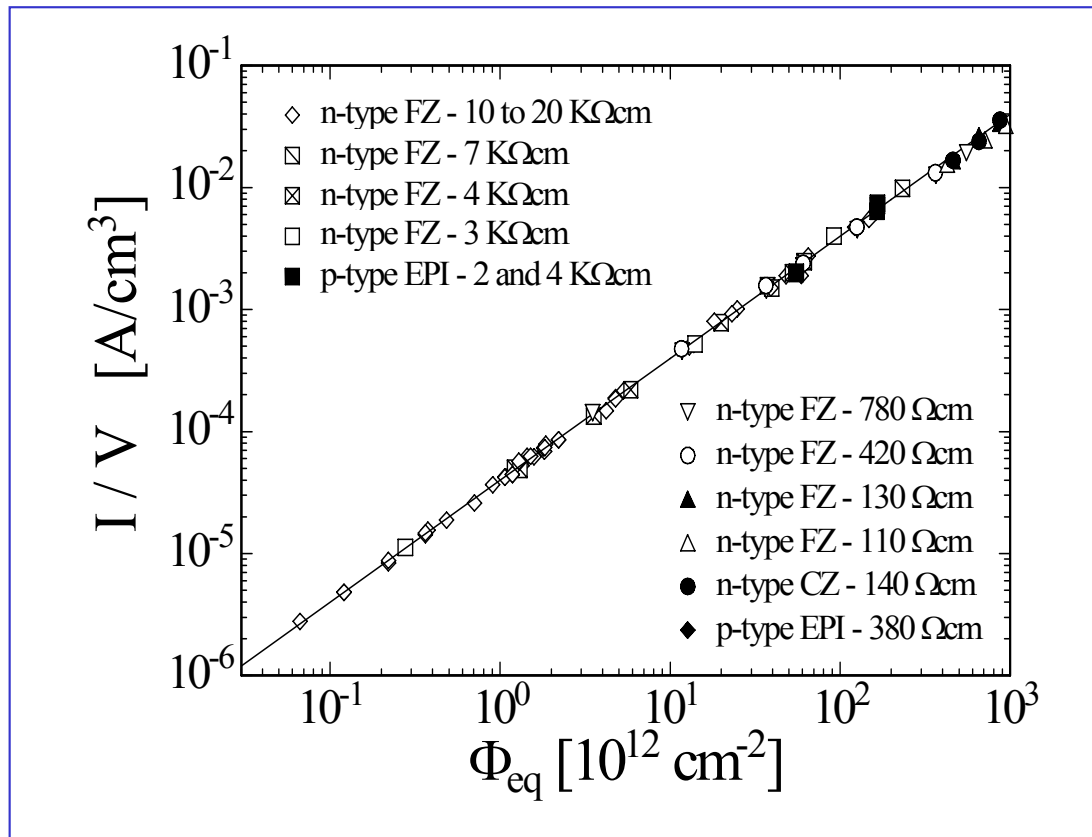
Effetti macroscopici dovuti all'irraggiamento (Si)

1. Analisi della regione svuotata

- a. Aumento della corrente di fuga con la fluenza di irraggiamento

$$\frac{I_{dep}}{Volume} = \alpha \cdot \Phi$$

$$\alpha = 4 \cdot 10^{-17} \text{ A / cm}$$

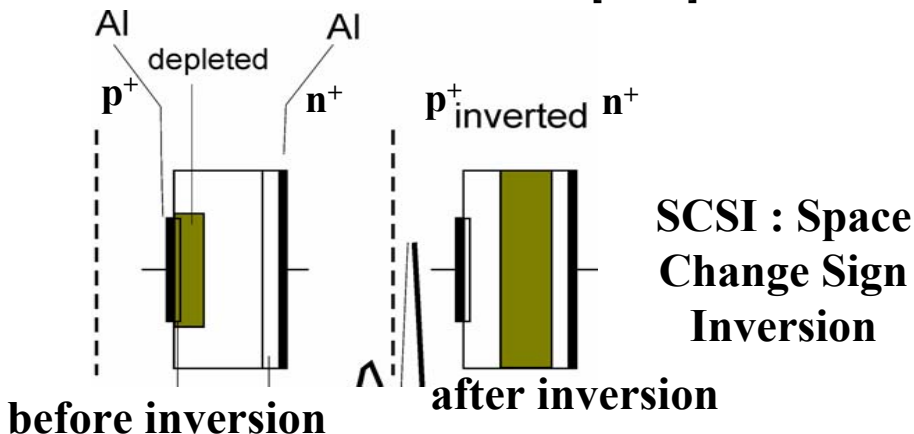
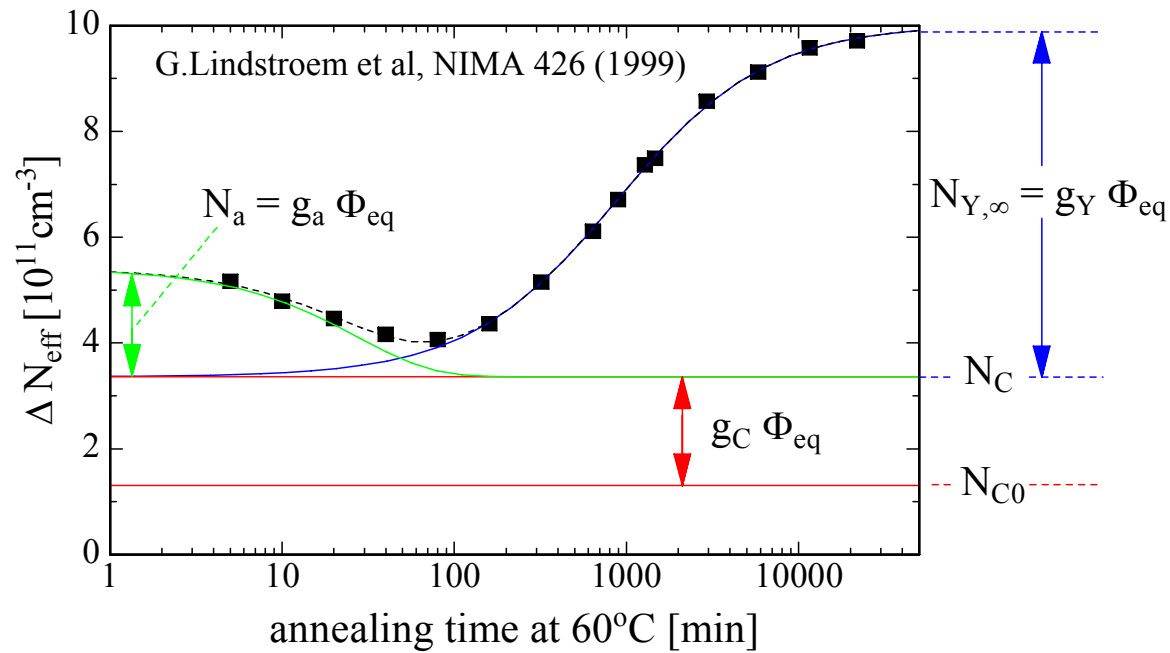
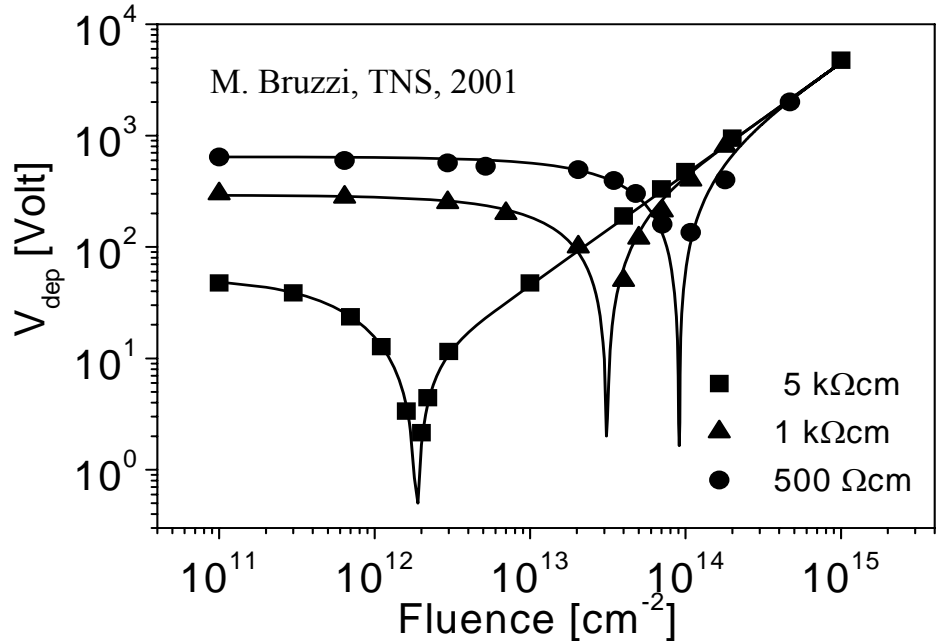


α independent of Φ_{eq} and impurities \Rightarrow used for fluence calibration
(NIEL-Hypothesis)

b. Variazione di V_{dep} e N_{eff} con la fluenza

$$\Delta N_{eff}(\Phi) = |N_{C0}(1 - e^{-c\Phi}) - \beta \cdot \Phi|$$

Produzione di difetti di tipo accettore
Rimozione/compensazione drogante superficiale



- **Short term:** “Beneficial annealing”
- **Long term:** “Reverse annealing”
time constant : ~ 500 years (-10°C)
~ 500 days (20°C)
~ 21 hours (60°C)

Decrease of the Charge Collection Efficiency

Limited by:

- Partial depletion
- Trapping at deep levels
- Type inversion

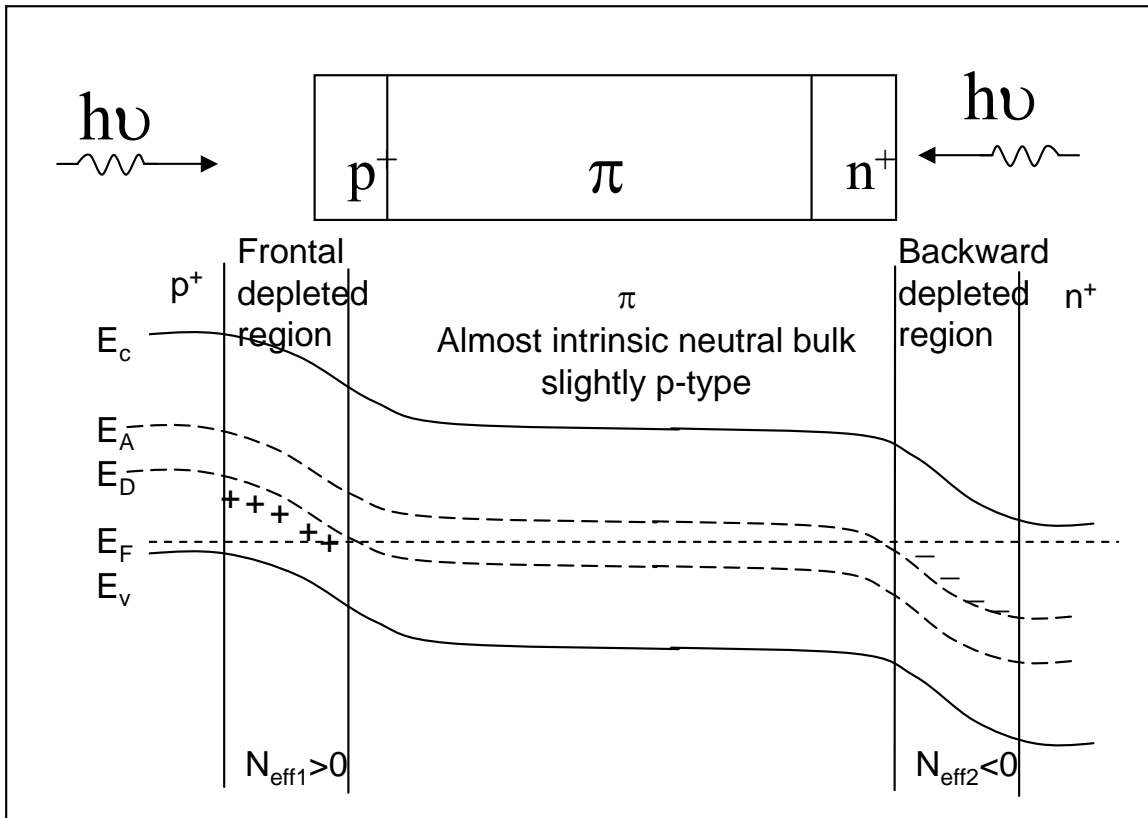
Collected Charge:

$$Q = Q_0 \cdot \epsilon_{dep} \cdot \epsilon_{trap}$$

$$\epsilon_{dep} = \frac{d}{W} - \frac{\tau_c}{\tau_t}$$

W: total thickness
d: Active thickness
 τ_c : Collection time
 τ_t : Trapping time

$$\epsilon_{trap} = e^{-\frac{\tau_t}{\tau_c}}$$



Appearance of a Double Junction at electrodes

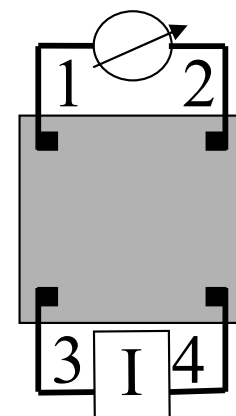
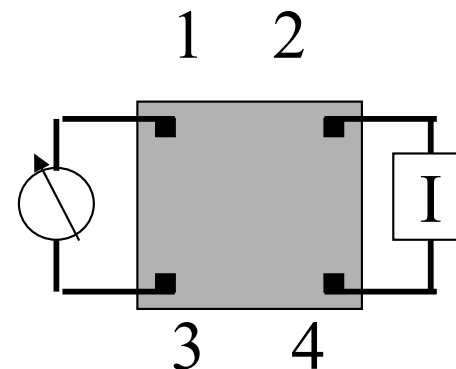
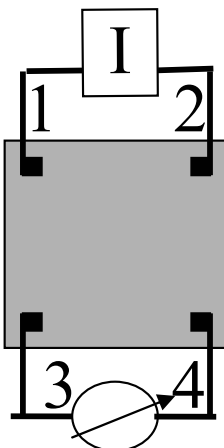
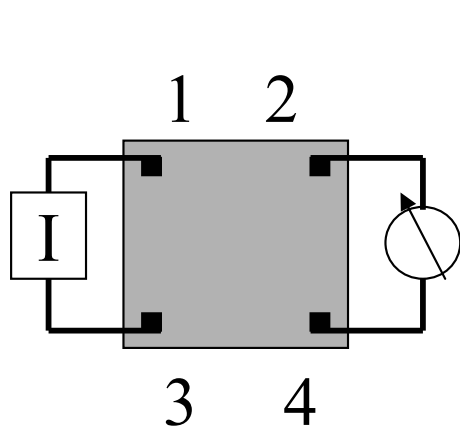


Double level model: Acceptor in second half – Donor in first half of bandgap originate the double junction. Levels are neutral in bulk, ionised close to contacts .

M. Bruzzi, TNS, 2001

2. Analisi della regione neutra

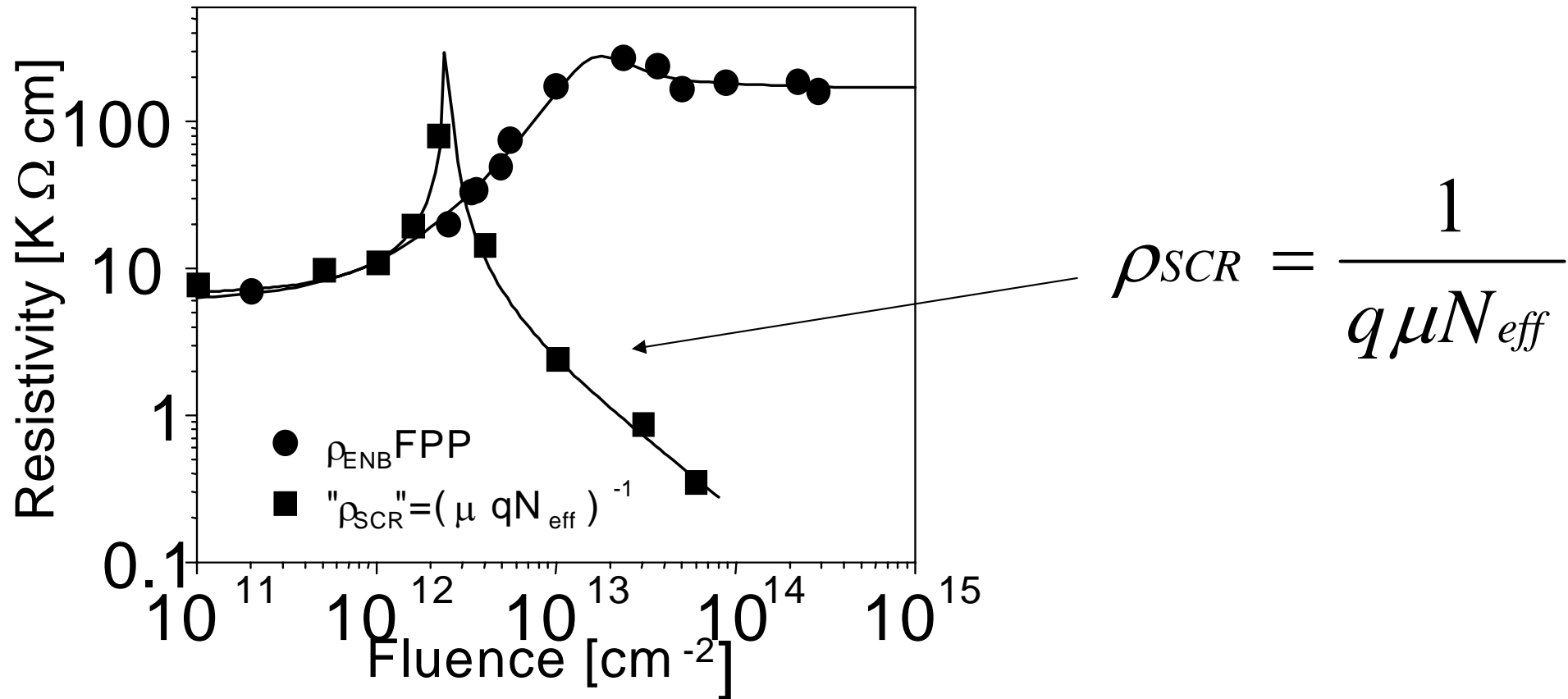
a. Misura della resistività con tecnica delle quattro punte



$$\rho = \frac{1}{q\mu_p(p + z \cdot n)}$$

$$z = \mu_n/\mu_p$$

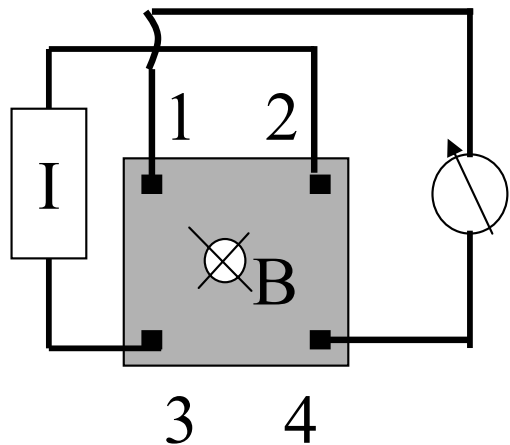
Emerge la **discrepanza tra resistività in regione neutra** (dovuta ai portatori liberi nella regione neutra) e **resistività apparente determinata attraverso N_{eff}** (concentrazione della carica fissa nella regione svuotata). L’irraggiamento provoca l’aumento della resistività di bulk per effetto della rimozione dei droganti superficiali indotta dall’irraggiamento e per la compensazione dovuta ai difetti profondi.



$$\rho_{SCR} = \frac{1}{q \mu N_{eff}}$$

b. Misura del coefficiente di Hall per la determinazione del tipo di portatori nella regione neutra

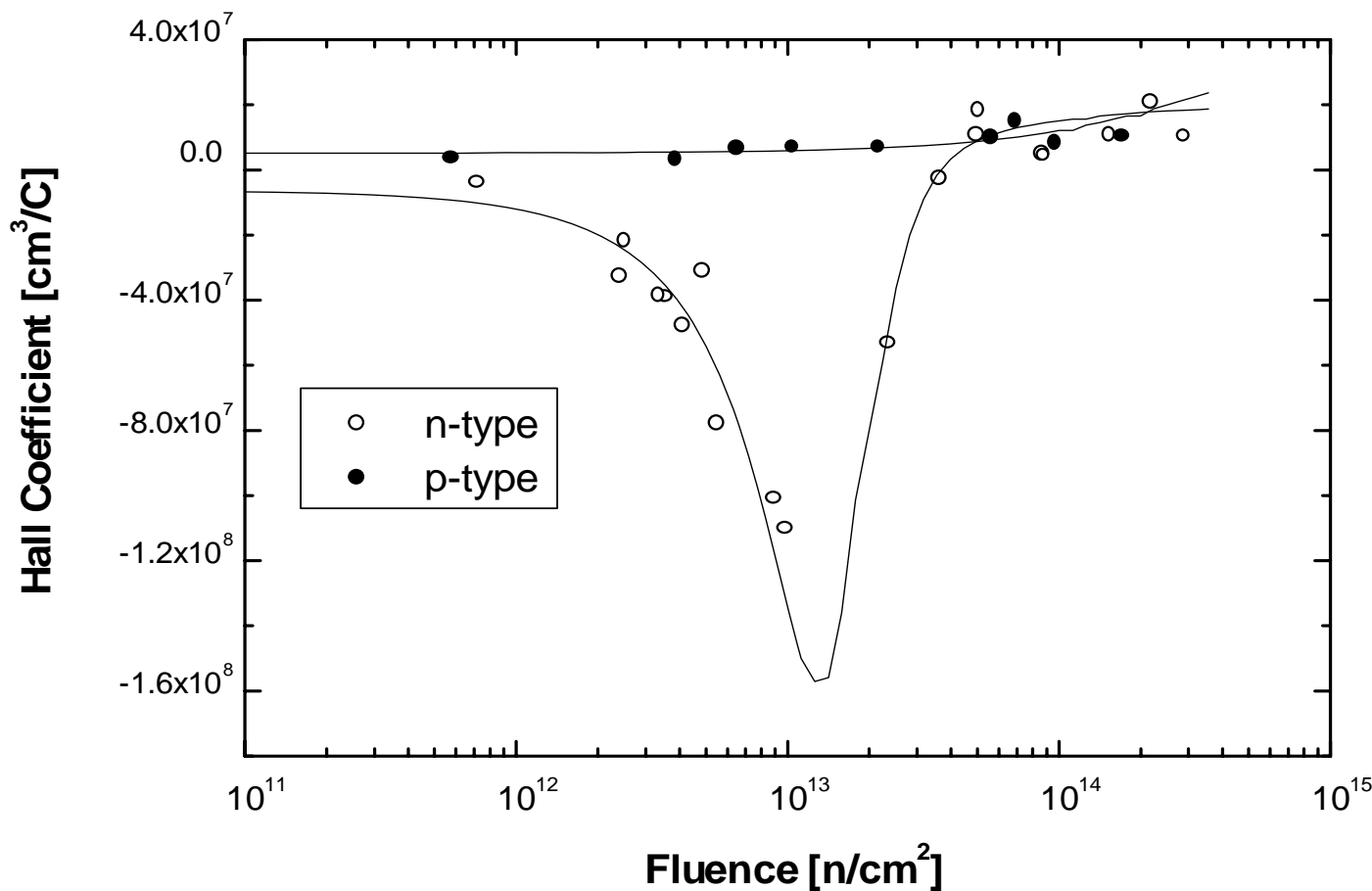
$$V_{\text{Hall}} = R_H J_x B_z h$$



$$R_H = r_H \cdot \frac{p - z^2 \cdot n}{q \cdot (p + z \cdot n)^2}$$

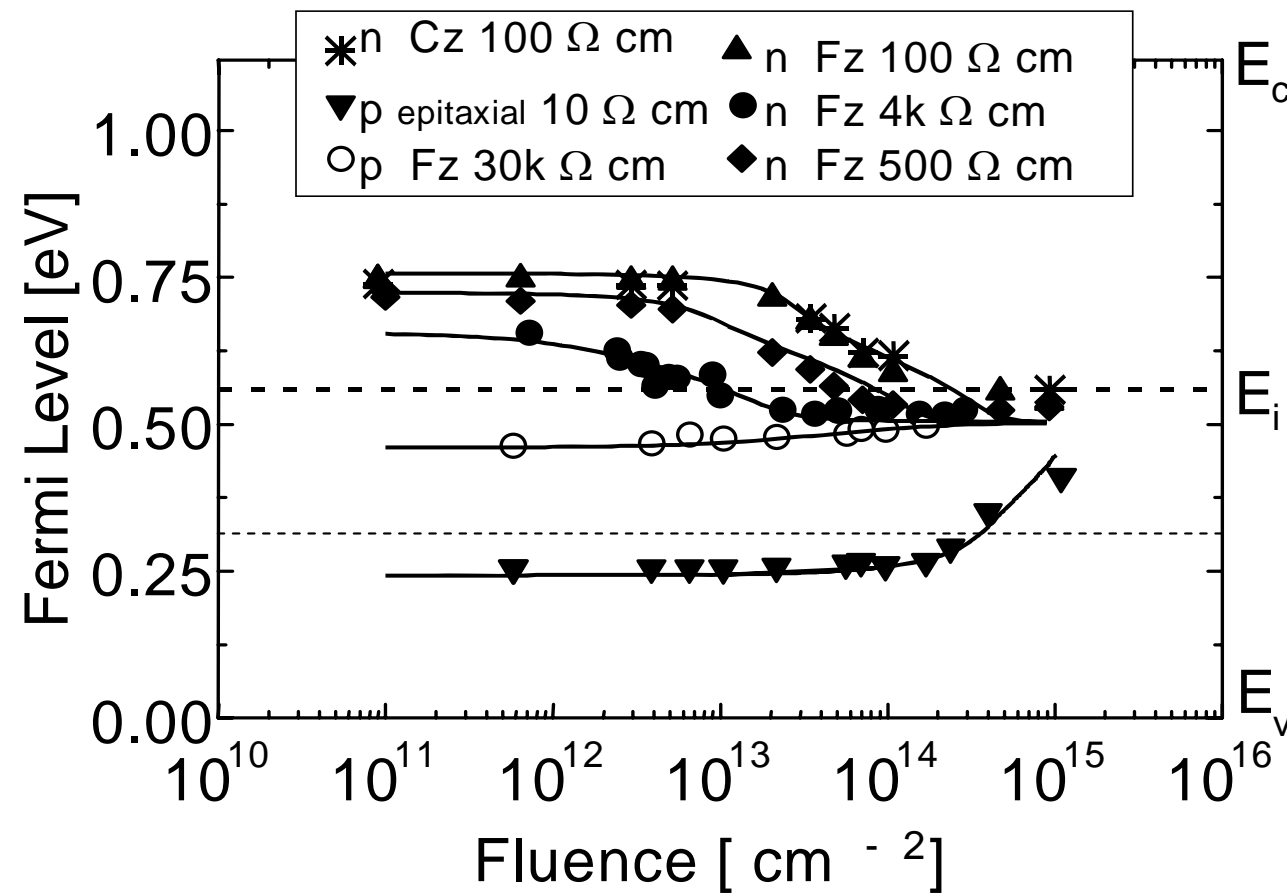
$$z = \mu_n / \mu_p$$

Misura del coefficiente di Hall per la determinazione del tipo di conducibilità



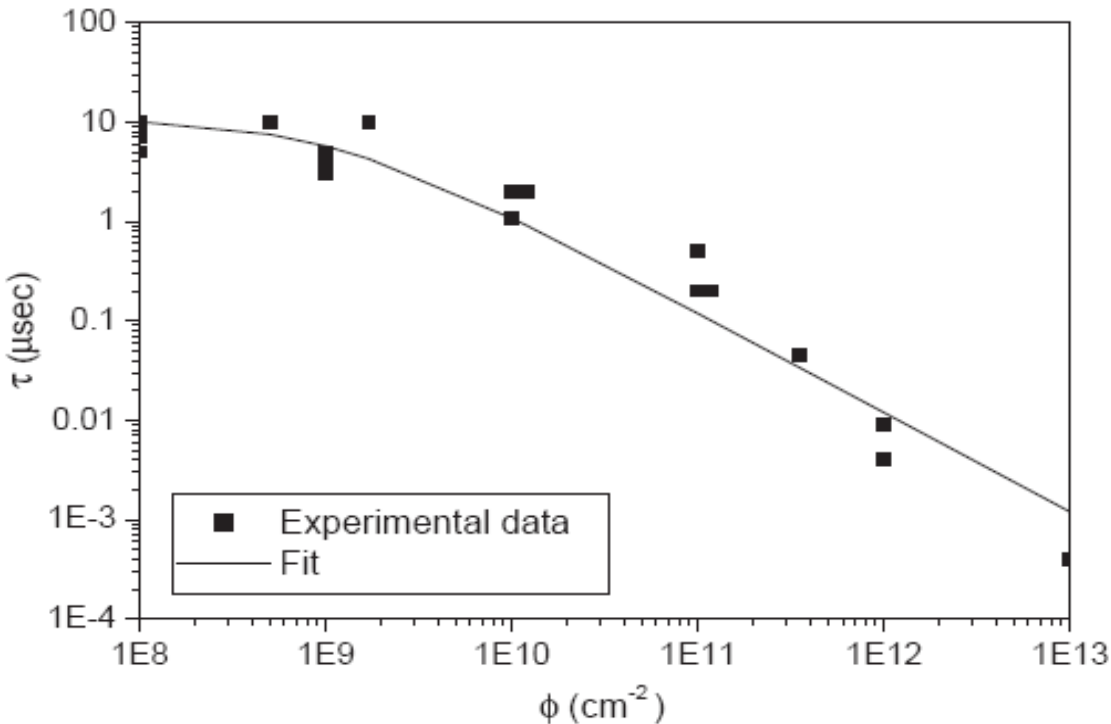
Il silicio inizialmente sia di tipo n che p, si presenta dopo irraggiamento come un materiale quasi intrinseco, debolmente di tipo p: π

Combinando i risultati ottenuti per resistività ed effetto Hall si determina la posizione del livello di Fermi in funzione della fluenza di irraggiamento.



Tutti i materiali a Si investigati mostrano ad elevata fluenza il pinning del livello di Fermi a $E_v + 0.5 \text{ eV}$

c. Degrado della vita media dei portatori minoritari



$$\frac{1}{\tau} = \frac{1}{\tau_0} + k_\tau \phi,$$

Per protoni da 10MeV

$$k_\tau = (1.52 \pm 0.05) \times 10^{-11} \mu \text{s}^{-1} \text{ cm}^2$$

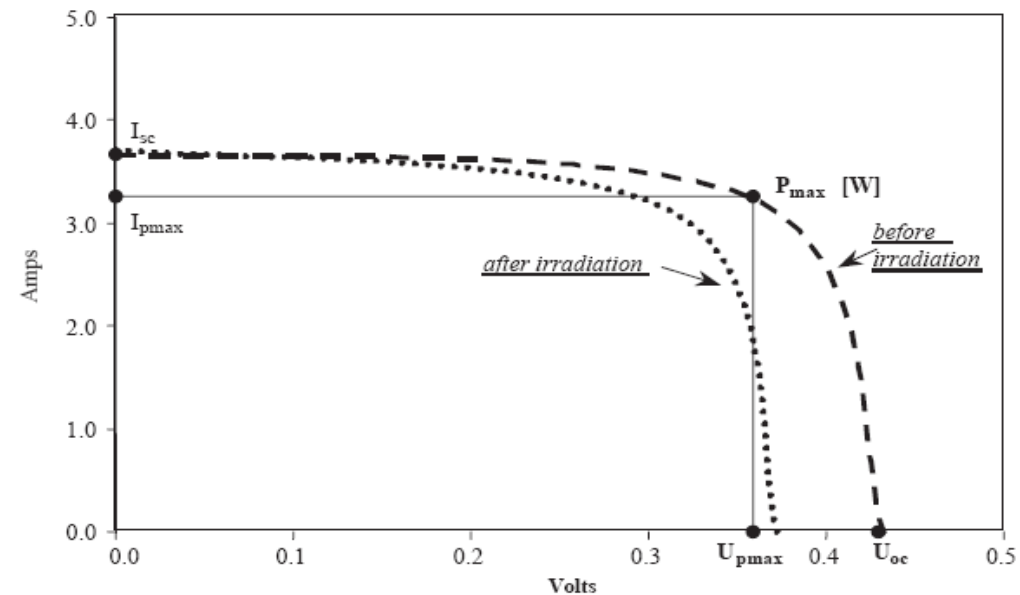
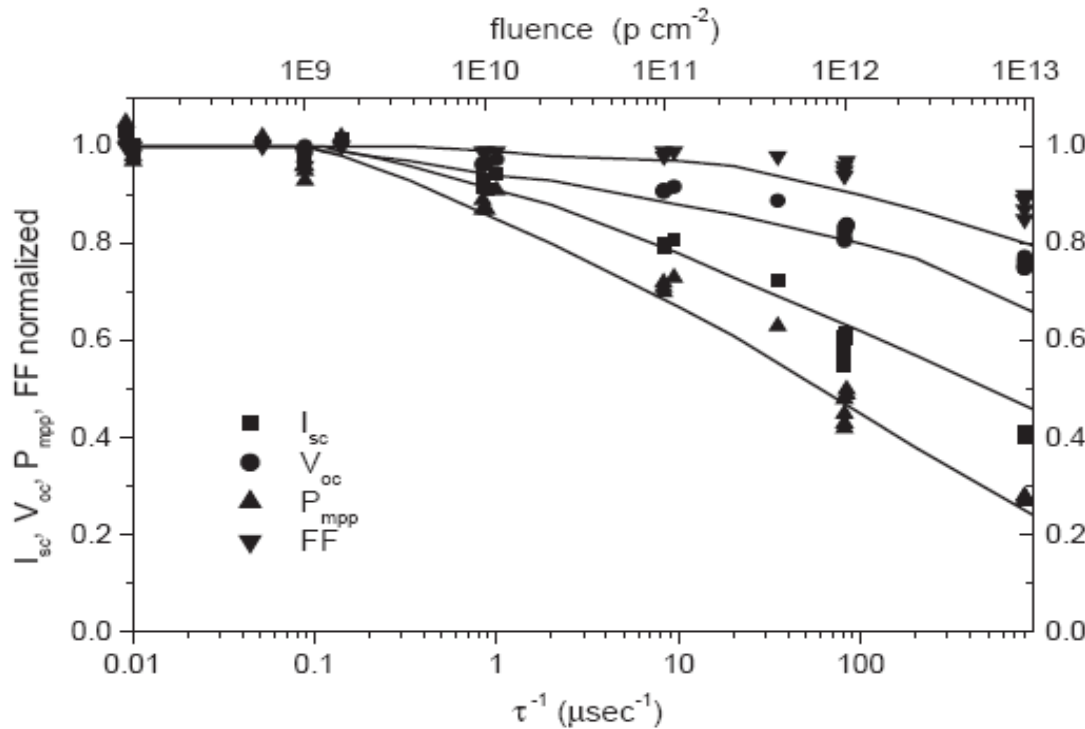
Convertendo a L, lunghezza di diffusione dei minoritari

$$L = \sqrt{D \cdot \tau} \quad \text{si ha:} \quad k_L = (5.6 \pm 0.2) \times 10^{-7}$$

10 MeV protons produces a 3000 times larger equivalent damage compared to 1 MeV electrons

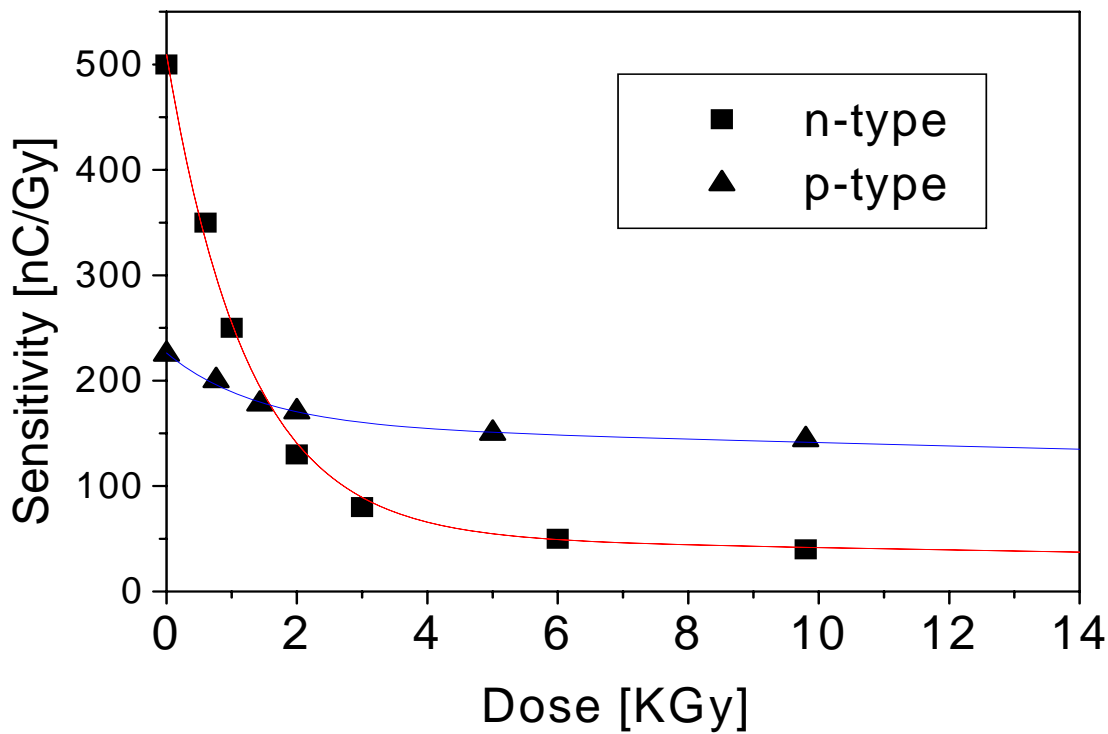
Radiation Damage in Si Solar cells

Degrado dei parametri operativi della cella solare interpretato come effetto della diminuzione della vita media dei portatori minoritari



Dosimetri per radioterapia clinica

sensibilità fortemente dipendente dalla dose accumulata



G.Rikner and E.Grusell, Effects of Radiation damage on p-type silicon detectors, Phys. Med. Biol. 1983, 28, 11, 1261-1267

$$s(D) = c_1 \cdot (1 - \alpha \cdot D) + c_2 \cdot \exp(-\beta \cdot D) \quad D = \text{Dose}$$

→ E' necessario calibrare il dosimetro ogni ~25Gy

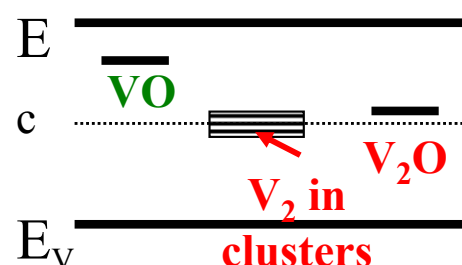
Material Engineering

Oxygen Enrichment for Radiation Hardening

RD48 (ROSE) CERN Collaboration

Main Hypothesis: Oxygen sink of vacancies

V-O_i complex concentration increase ~~—~~ reduction of deeper levels
mainly divacancy related



1964 Significant radiation hardening for Co⁶⁰ γ -irradiation by increasing the oxygen concentration (CZ Si)

T.Nakano, Y.Inuishi, effects of dosage and impurities on radiation damage of carrier lifetime in silicon, J.Phys. Soc., 19, 851-858,(1964)

1966 Neutron-induced degradation independent of the oxygen concentration (CZ Si)

O.L.Curtis Jr., Effects of oxygen and dopant on lifetime in neutron-irradiated silicon, IEEE Trans. Nucl. Sci. NS-13, 6, 33-40 (1966).

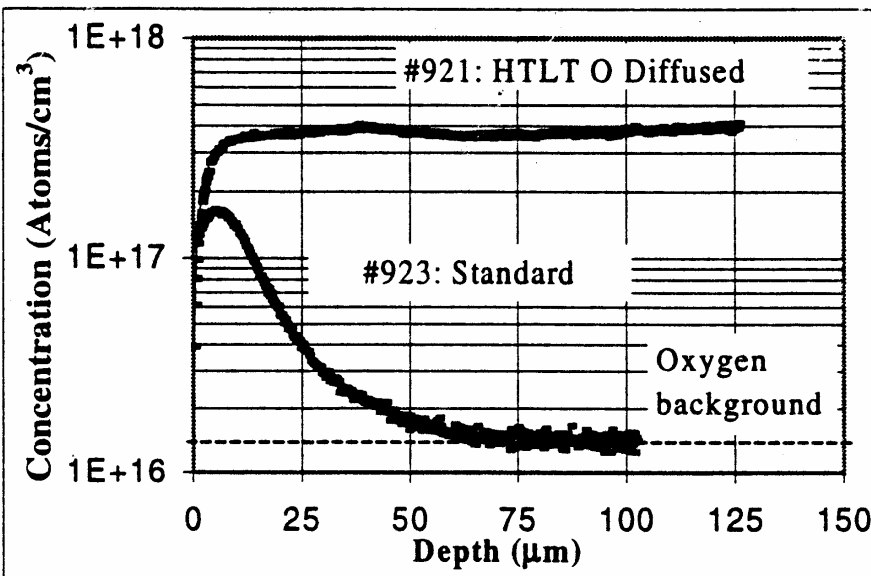
Mara Bruzzi, Danno da radiazione in semiconduttori

Scuola Nazionale rivelatori ed elettronica per fisica delle alte energie , astrofisica 21 Aprile 2009, Legnaro, Italy

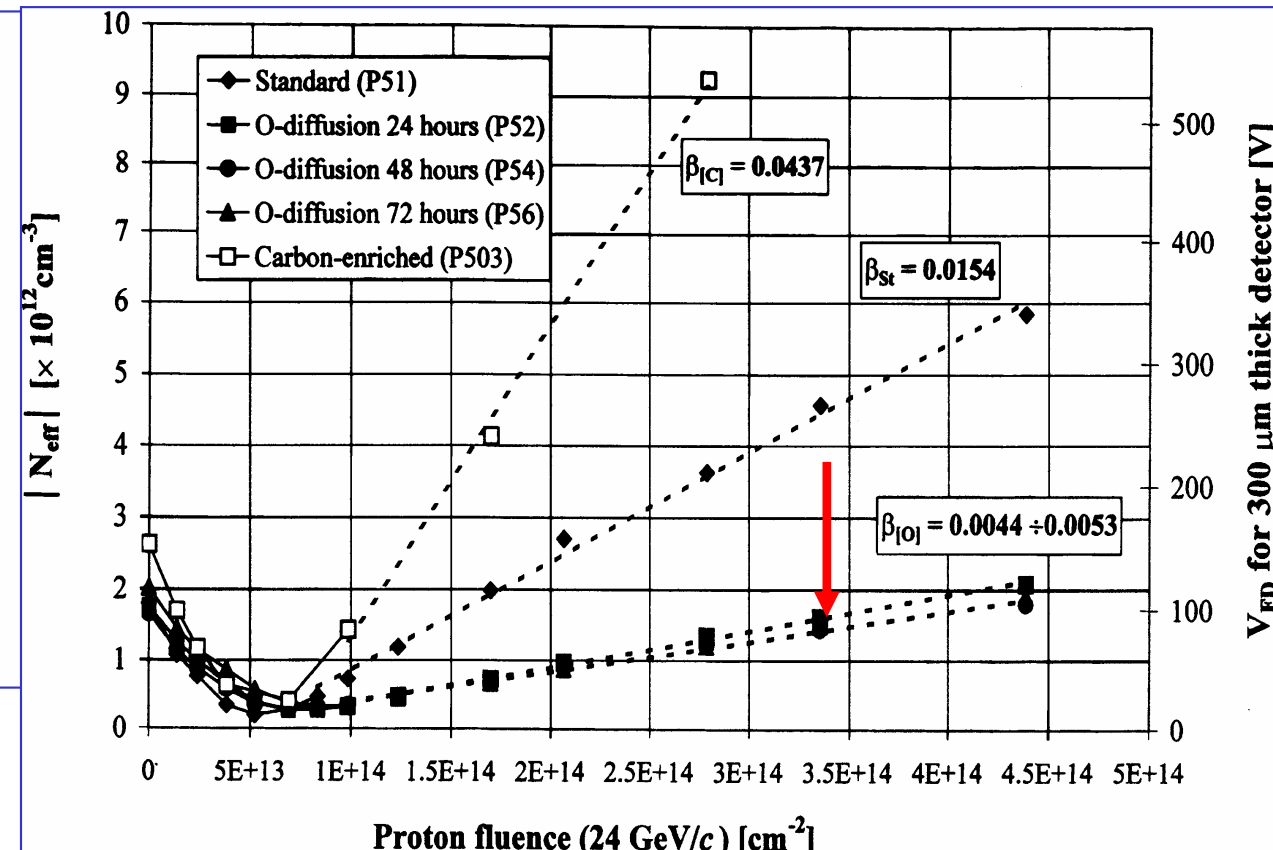
Decrease of N_{eff} and V_{dep} changes after γ and p irradiation

Diffusion oxygenated Float Zone Silicon

Oxygen enrichment at BNL (1992) $[O_i] \sim 5 \times 10^{17} \text{ cm}^{-3}$ in pure FZ Si



Z.Li et al. IEEE Trans. Nucl. Sci.
42, 4, 219-223 (1995)



A.Ruzin, Cern RD48 Coll. NIM A 447 (2000), 116-125



The RD50 CERN Collaboration

Development of Radiation Hard Semiconductor Devices for High Luminosity Colliders

- **Collaboration formed in November 2001 - <http://www.cern.ch/rd50>**
- **Experiment approved as RD50 by CERN in June 2002**
- **Main objective:**

Development of ultra-radiation hard semiconductor detectors for the luminosity upgrade of the LHC to $10^{35} \text{ cm}^{-2}\text{s}^{-1}$ ("Super-LHC").

Challenges: - Radiation hardness up to 10^{16} cm^{-2} required
 - Cost effectiveness

- **Presently 250 Members from 50 Institutes**

Belgium (Louvain), Canada (Montreal), Czech Republic (Prague (2x)), Finland (Helsinki (2x), Oulu), Germany (Berlin, Dortmund, Erfurt, Halle, Hamburg, Karlsruhe), Greece (Athens), Israel (Tel Aviv), Italy (Bari, Bologna, Florence, Milano, Modena, Padova, Perugia, Pisa, Trento, Trieste, Turin), Lithuania (Vilnius), Norway (Oslo (2x)), Poland (Warsaw), Romania (Bucharest (2x)), Russia (Moscow (2x), St.Petersburg), Slovenia (Ljubljana), Spain (Barcelona, Valencia), Sweden (Lund) Switzerland (CERN, PSI), Ukraine (Kiev), United Kingdom (Exeter, Glasgow, Lancaster, Liverpool, London, Sheffield, University of Surrey), USA (Fermilab, Purdue University, Rutgers University, Syracuse University, BNL, University of New Mexico)

Different kind of Si materials investigated by RD50

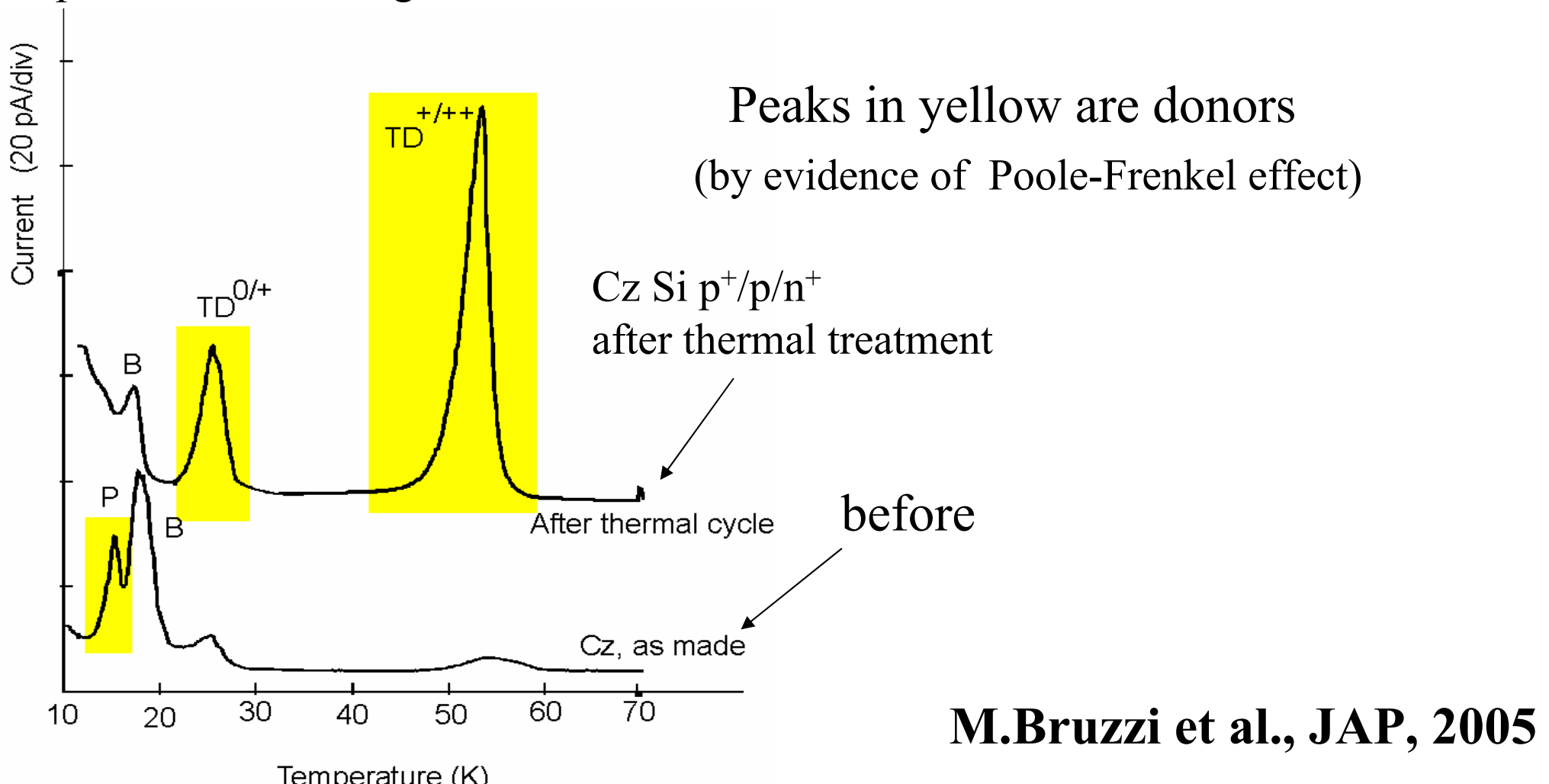
Material	Symbol	$\rho \Omega \text{cm}$	$[\text{O}_i] \text{ cm}^{-3}$
Standard n - or p - type FZ	STNFZ	$1-7 \cdot 10^3$	$< 5 \cdot 10^{16}$
Diffusion Oxygenated FZ p or n - type	DOFZ	$1-7 \cdot 10^3$	$\sim 1-2 \cdot 10^{17}$
Epi- layer 50 μm on CZ n -type ITME	EPI	50-100	substrate: $1 \cdot 10^{18}$
Czochralski Sumitomo, Japan	CZ	$1.2 \cdot 10^3$	$\sim 8-9 \cdot 10^{17}$
Magnetic Czochralski Okmetic Finland	MCZ	$1.2 \cdot 10^3$	$\sim 5-9 \cdot 10^{17}$

Czochralski Si

- Very high Oxygen content 10^{17} - 10^{18}cm^{-3} (**Grown in SiO_2 crucible**)
- High resistivity ($> 1 \text{K}\Omega\text{cm}$) available only recently (**Magnetic CZ technology**)
- CZ wafers cheaper than FZ (**RF-IC industry got interested**)

Defects related to Oxygen: Thermal donors and Oxygen Dimers

TDs are small clusters of 4 atoms formed at the early stages of oxygen aggregation. Only silicon with an oxygen concentration $[O_i]$ higher than 10^{17} cm^{-3} exhibits significant content of these defects. TDs in Cz Si can be activated by heating the material at temperatures in the range 400-500°C.

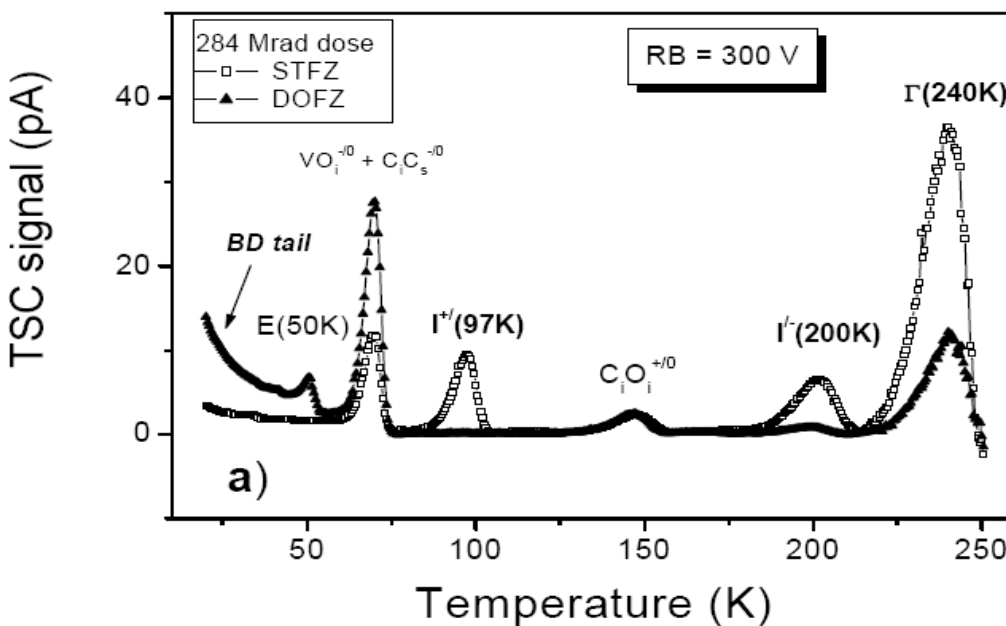


γ Co⁶⁰ irradiation: beneficial behavior of DOFZ

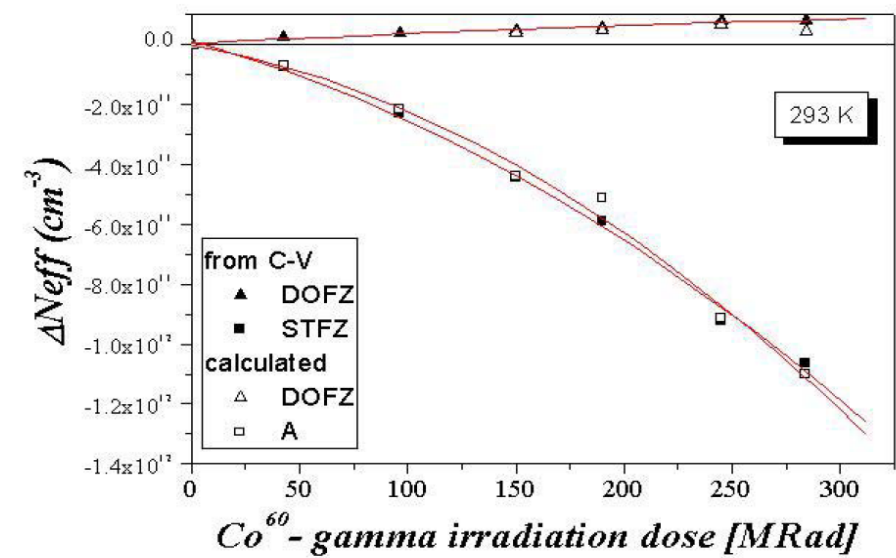
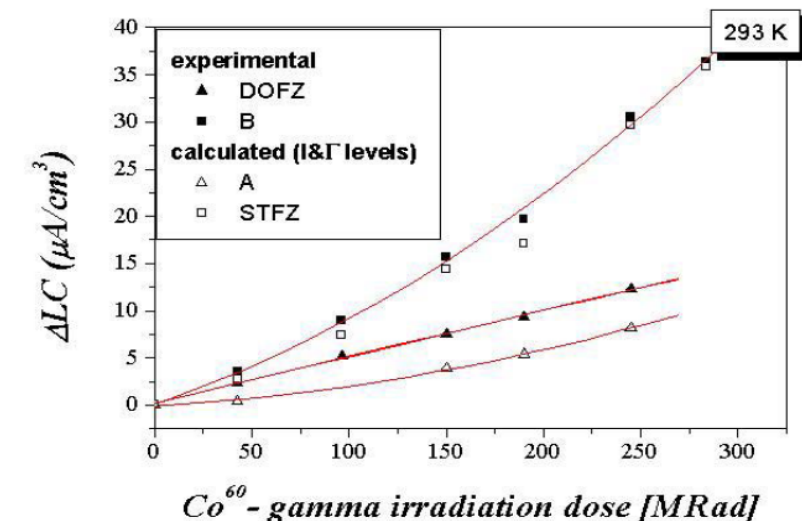
To investigate only point defects; Main focus on differences between standard and oxygen enriched material and impact of the observed defect generation on pad detector properties.

Beneficial oxygen effect consists in:

- (a) suppressing deep acceptors responsible for the type inversion effect in oxygen lean material. So called I and Γ close to midgap acceptor like levels and are generated in higher concentrations in STFZ silicon than in DOFZ;
- (a) shallow donors (BD) creation as well;

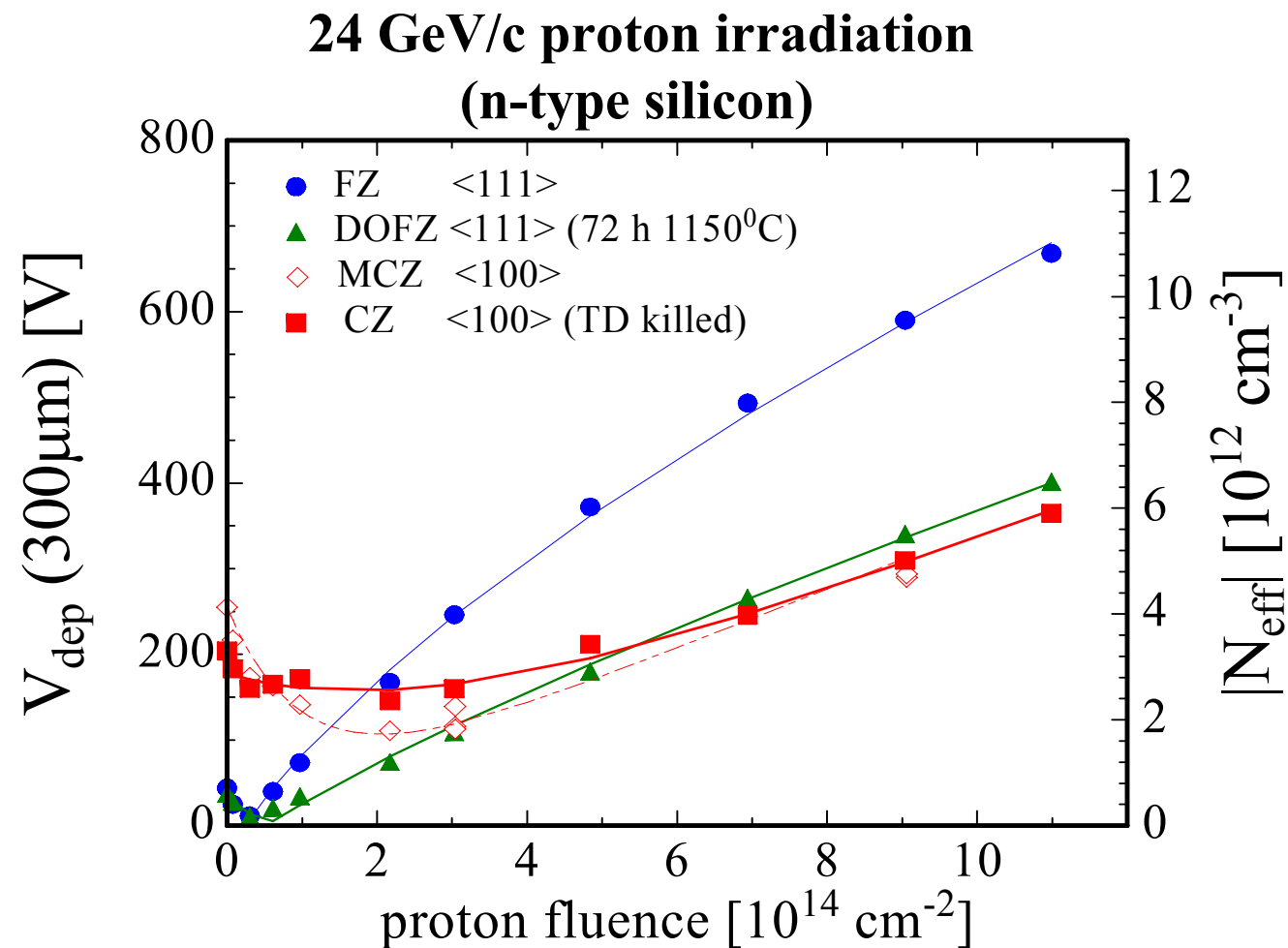


[I. Pintilie, APL, 82, 2169, March 2003]



Proton irradiation: comparison of FZ, DOFZ, Cz and MCz Silicon

- Strong differences in V_{dep}
 - Standard FZ silicon
 - Oxygenated FZ (DOFZ)
 - CZ silicon and MCZ silicon
- Strong differences in internal electric field shape
(type inversion, double junction,...)
 - Red arrow pointing down
- Different impact on pad and strip detector operation!



- Common to all materials (after hadron irradiation):
 - reverse current increase
 - increase of trapping (electrons and holes) within $\sim 20\%$

proton irradiated silicon detectors

Levels responsible for depletion voltage after 23 GeV proton irradiation:

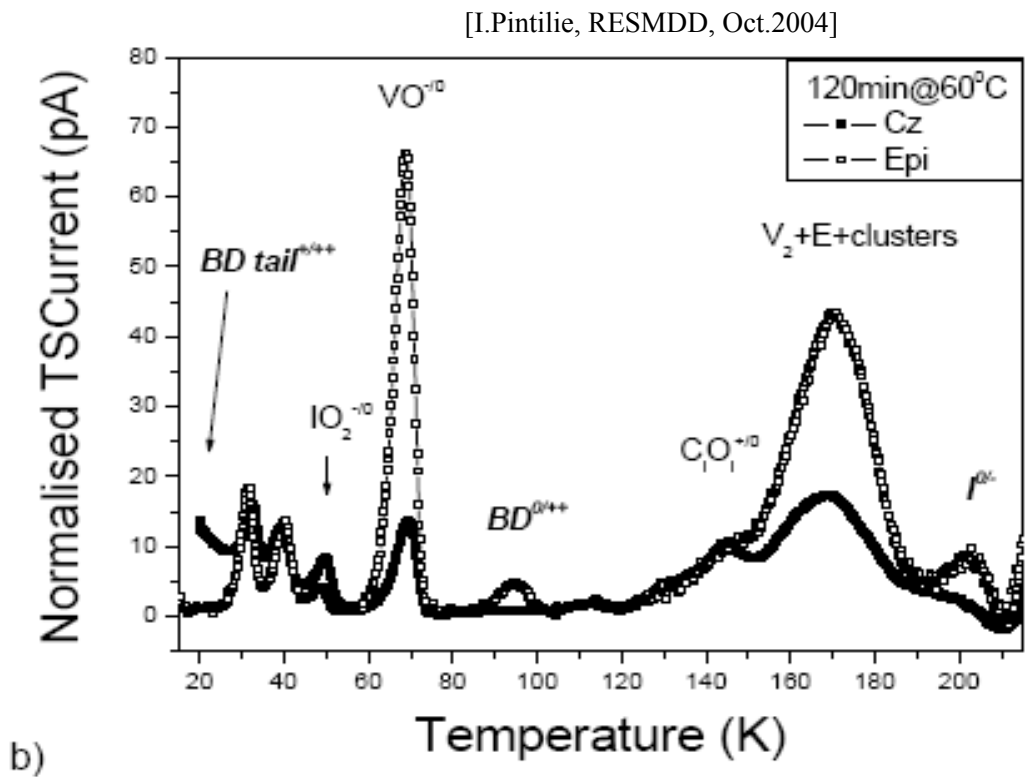
Almost independent of oxygen content:

- Donor removal
- “Cluster damage” \Rightarrow negative charge

Influenced by initial oxygen content:

- deep acceptor level at $E_C - 0.54\text{eV}$
(good candidate for the V_2O defect)
 \Rightarrow negative charge

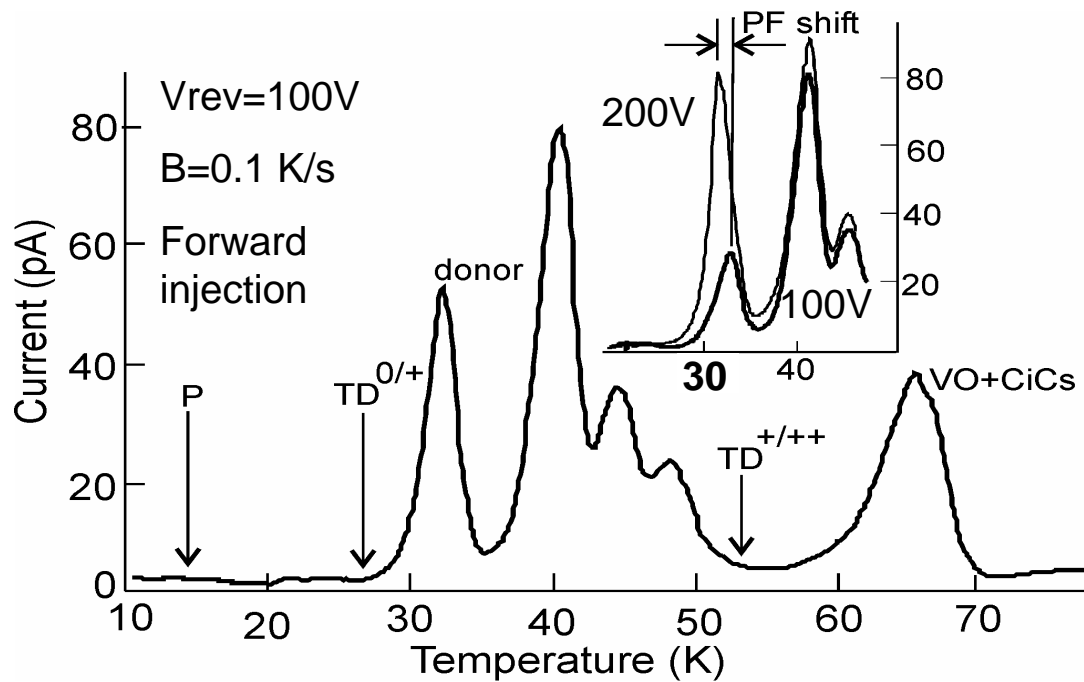
- Influenced by initial oxygen dimer content (?):
- BD-defect: **bistable shallow thermal donor**
(formed via oxygen dimers O_{2i})
 \Rightarrow positive charge



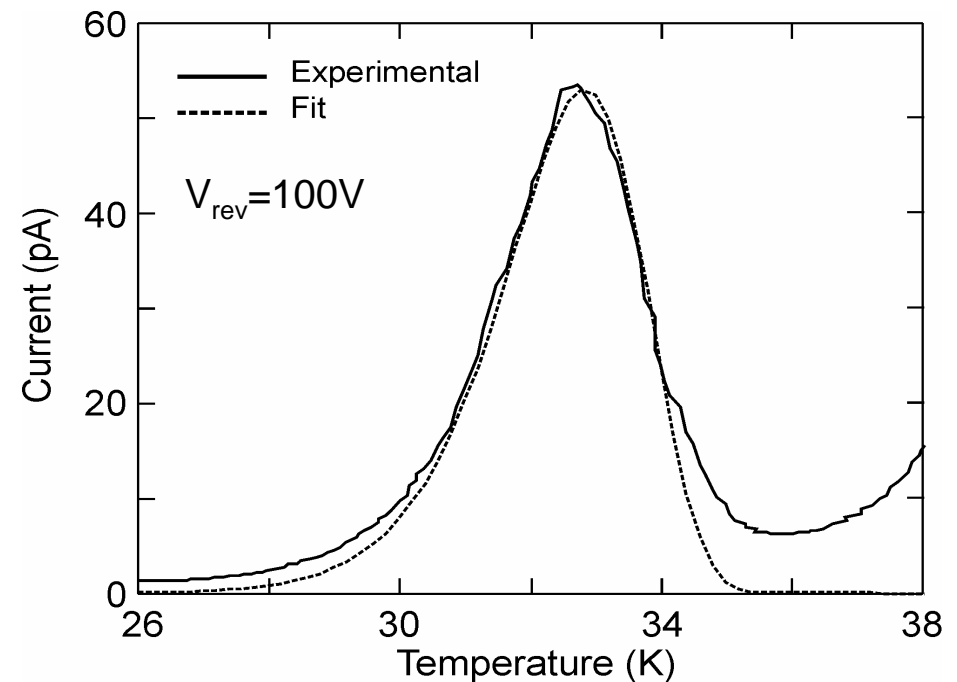
TSC after irradiation with 23 GeV protons with an equivalent fluence of $1.84 \times 10^{14} \text{ cm}^{-2}$ recorded on Cz and Epi material after an annealing treatment at 600C for 120 min.

Shallow donor levels after proton irradiation

- 1) No TDs.
- 2) Shallow Donor close to 30 K peak (PF shift evidences its donor-like nature)



M. Bruzzi et al., NIM A 552 (2005) pp. 20-26.
N-type MCz Si – SMART
24GeV/c p up to $4 \times 10^{14} \text{ p/cm}^2$
Annealing: 1260min at 60°C



M. Scaringella et al.
NIM A 570 (2007) 322–329

Recent Literature on Defects in neutron irradiated silicon

V_2 has two charge states at 0.24 and 0.43 eV below E_c corresponding to 135 K and 233 K transitions. **A large 233 K peak is the hallmark of neutron-damaged silicon, related to clusters;** electron irradiation, which produces more uniform displacement damage, shows two nearly equal peaks at 135 and 233 K.

Two bistable configurations of the defects.

1. either immediately after irradiation or after forward bias (12.5 A/cm^2 at 300 K for 20 min). Increase in the 233 K peak and appearance of the 195 K peak/shoulder. After neutron , but not electron irr., decrease in the shallow V_2 peak at 135 K.
2. after sample at 350 K for 60 min either shorted or reverse biased or after the sample has been at room temperature for months. Lower 233 K peak, a much lower 0.36 eV trap signature, and a larger shallow V_2 peak (neutron irr.)

Change in the $V_2^{=/-}$ intensity (neutron irr.) explained as partial filling of the level due to band bending within a cluster.

R. M. Fleming, C. H. Seager, D. V. Lang, E. Bielejec, and J. M. Campbell, APL, 90, 172105 2007

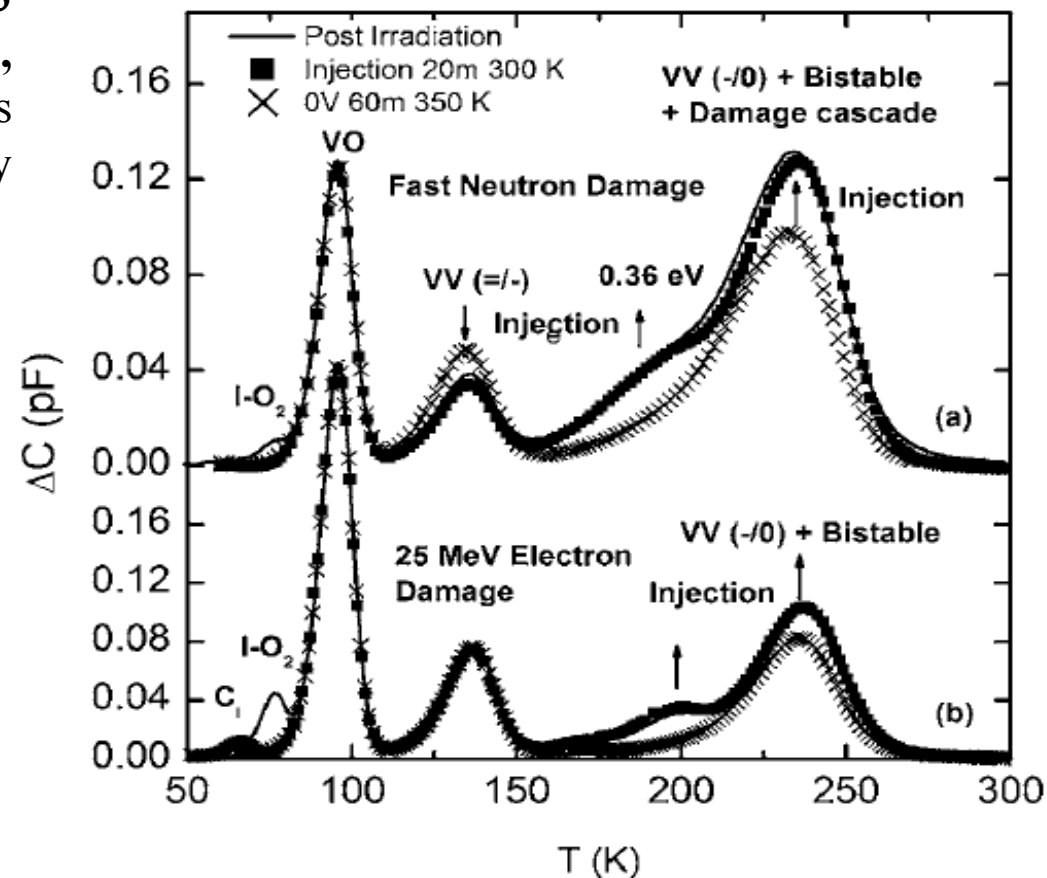
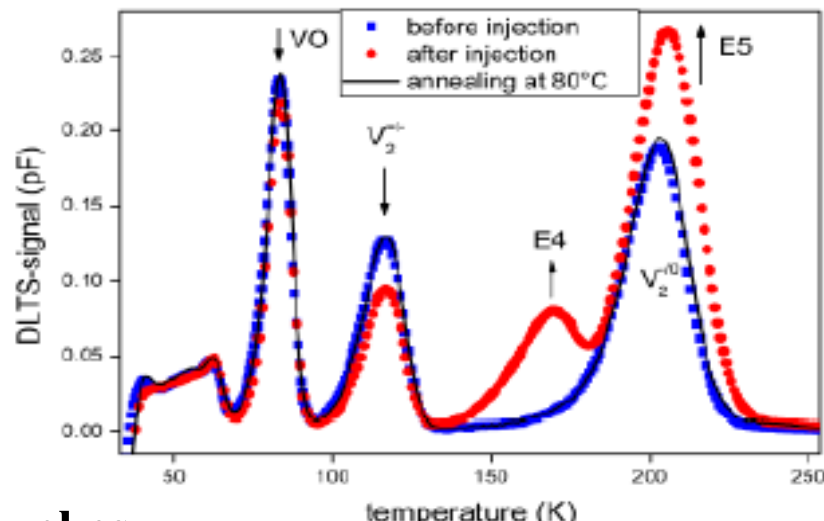


FIG. 1. DLTS of the base-collector diode of radiation damaged $n-p-n$ transistors. The DLTS spectrum can be cycled between two limiting cases, a higher defect state (immediately after irradiation or after forward bias at 300 K) and a lower defect state (after zero or reverse bias at 350 K). (a) Fast neutrons and (b) 25 MeV electrons.

Bistability of E4/E5

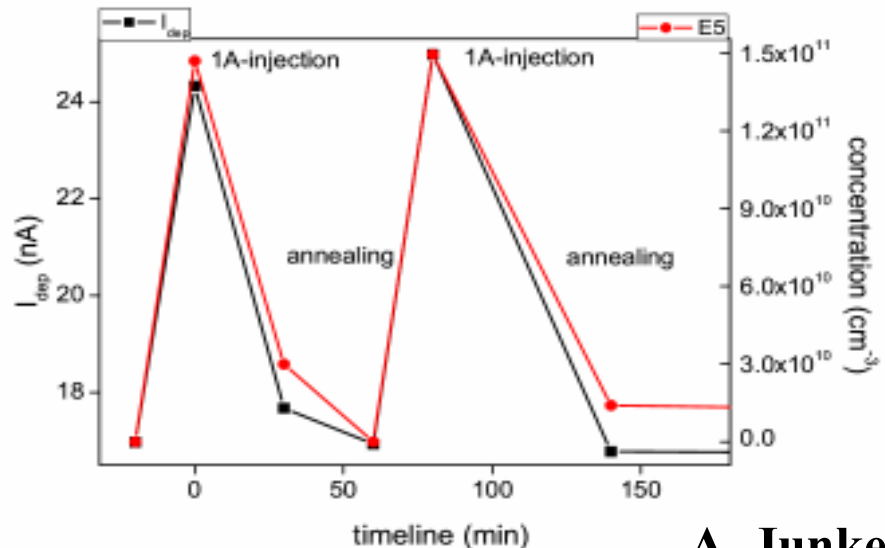


A. Junkes

Procedure:

- Pre-annealing at 200 °C for 30min before injection
- Injection 1 A forward current for 20 min
- Annealing at 80 °C for 60 min

E4/E5 can be totally recovered by injection of 1 A forward current



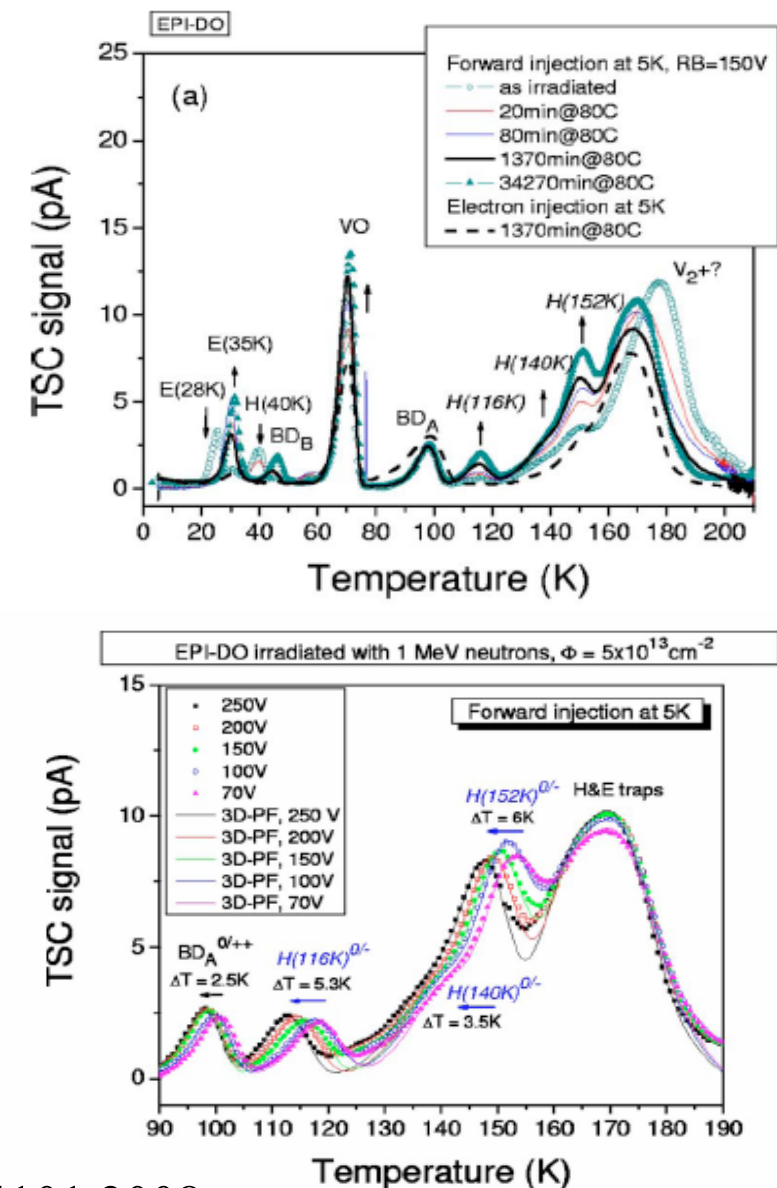
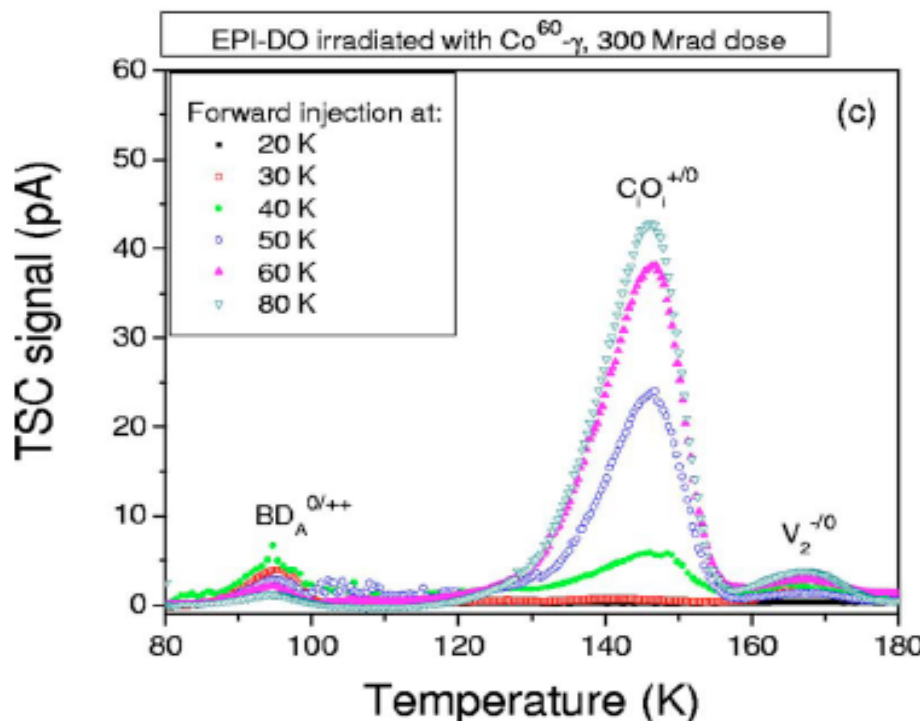
A. Junkes

Bistability of E4/E5 correlated with change of reverse current I_{dep}

First observation by R.M. Fleming et al., APL 90 (2007) 172105

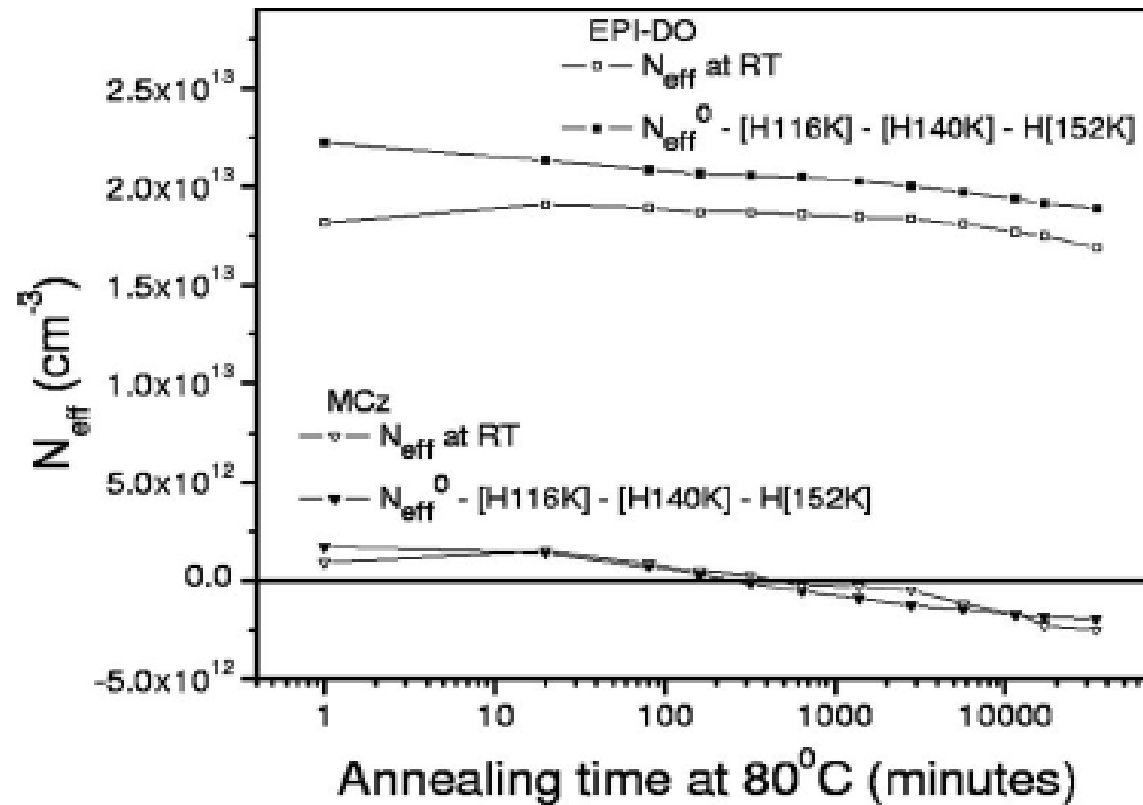
Cluster related hole traps as source for long term annealing

Hole traps H_{116} K, H_{140} K, and H_{152} K, cluster related defects (not present after γ -irradiation) observed in neutron irradiated *n*-type Si diodes during 80 °C annealing. To be observed by TSC it is necessary to deactivate C_iO_i , through filling with forward injection at very low initial temperature.



I. Pintilie, E. Fretwurst, and G. Lindström, APL **92**, 024101 2008

Hole traps $H116$ K, $H140$ K, and $H152K$ concentration in agreement with Neff changes during 80°C annealing, they are believed to be causing the long term annealing effects.



I. Pintilie, E. Fretwurst, and G. Lindström, APL **92**, 024101 2008

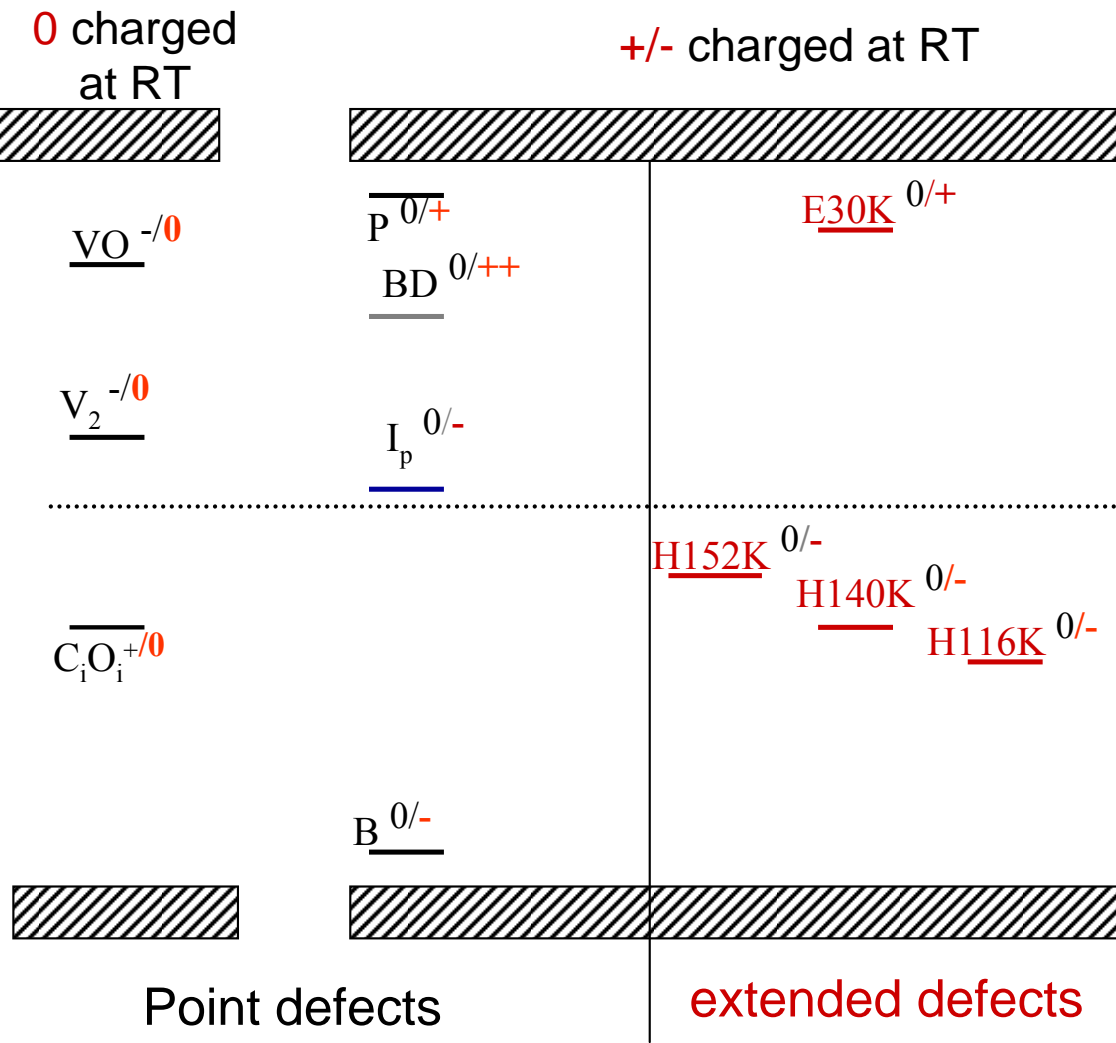
Summary – defects with strong impact on the device properties at operating temperature

Point defects

- $E_i^{BD} = E_c - 0.225 \text{ eV}$
 $\sigma_n^{BD} = 2.3 \cdot 10^{-14} \text{ cm}^2$
- $E_i^I = E_c - 0.545 \text{ eV}$
– $\sigma_n^I = 2.3 \cdot 10^{-14} \text{ cm}^2$
– $\sigma_{sp}^I = 2.3 \cdot 10^{-14} \text{ cm}^2$

Cluster related centers

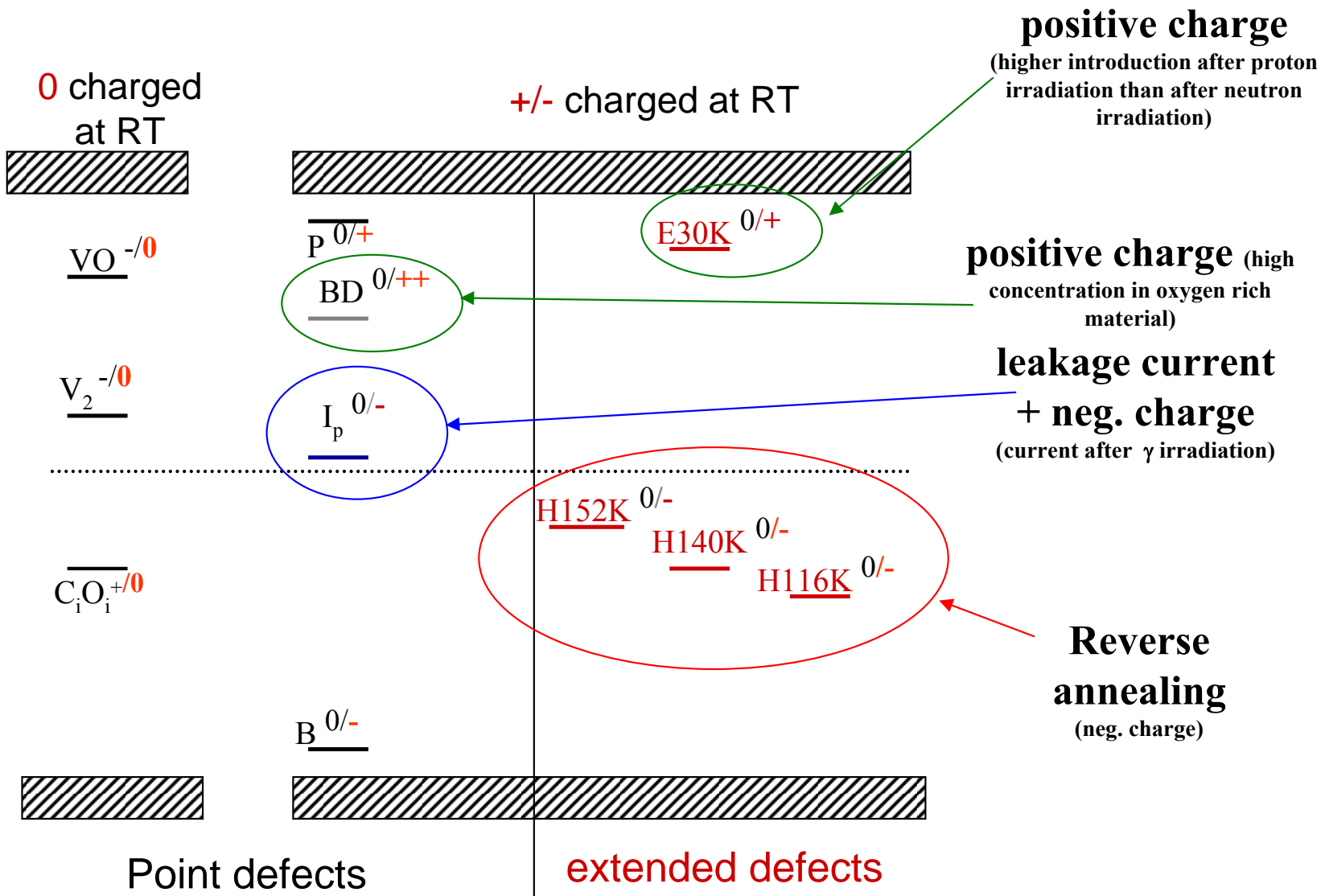
- $E_i^{116K} = E_v + 0.33 \text{ eV}$
- $\sigma_p^{116K} = 4 \cdot 10^{-14} \text{ cm}^2$
- $E_i^{140K} = E_v + 0.36 \text{ eV}$
- $\sigma_p^{140K} = 2.5 \cdot 10^{-15} \text{ cm}^2$
- $E_i^{152K} = E_v + 0.42 \text{ eV}$
- $\sigma_p^{152K} = 2.3 \cdot 10^{-14} \text{ cm}^2$
- $E_i^{30K} = E_c - 0.1 \text{ eV}$
- $\sigma_n^{30K} = 2.3 \cdot 10^{-14} \text{ cm}^2$



I.Pintilie, NSS, 21 October 2008, Dresden

Summary – defects with strong impact on the device properties at operating temperature

<u>Point defects</u>
• $E_i^{BD} = E_c - 0.225 \text{ eV}$
• $\sigma_n^{BD} = 2.3 \cdot 10^{-14} \text{ cm}^2$
• $E_i^I = E_c - 0.545 \text{ eV}$
– $\sigma_n^I = 2.3 \cdot 10^{-14} \text{ cm}^2$
– $\sigma_{sp}^I = 2.3 \cdot 10^{-14} \text{ cm}^2$
<u>Cluster related centers</u>
• $E_i^{116K} = E_v + 0.33 \text{ eV}$
• $\sigma_p^{116K} = 4 \cdot 10^{-14} \text{ cm}^2$
• $E_i^{140K} = E_v + 0.36 \text{ eV}$
• $\sigma_p^{140K} = 2.5 \cdot 10^{-15} \text{ cm}^2$
• $E_i^{152K} = E_v + 0.42 \text{ eV}$
• $\sigma_p^{152K} = 2.3 \cdot 10^{-14} \text{ cm}^2$
• $E_i^{30K} = E_c - 0.1 \text{ eV}$
• $\sigma_n^{30K} = 2.3 \cdot 10^{-14} \text{ cm}^2$



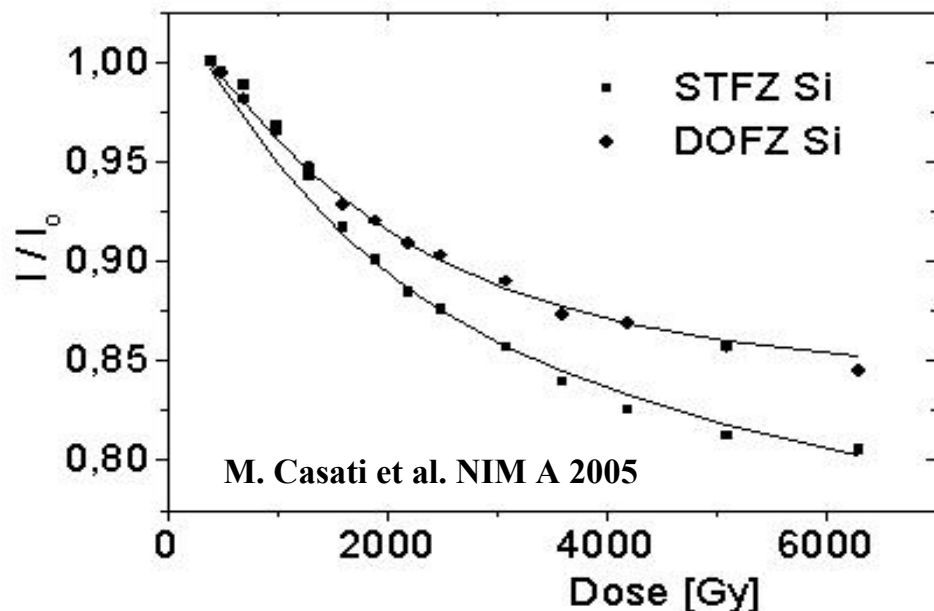
I.Pintilie, NSS, 21 October 2008, Dresden

Mara Bruzzi, Danno da radiazione in semiconduttori

Scuola Nazionale rivelatori ed elettronica per fisica delle alte energie , astrofisica 21 Aprile 2009, Legnaro, Italy

Material engineering concepts have been applied also to Silicon dosimeters for radiotherapy

Improved radiation hardness of DOFZ Si



Decrease in sensitivity with the accumulated dose due to the generation of a dominant trap acting as lifetime killer.

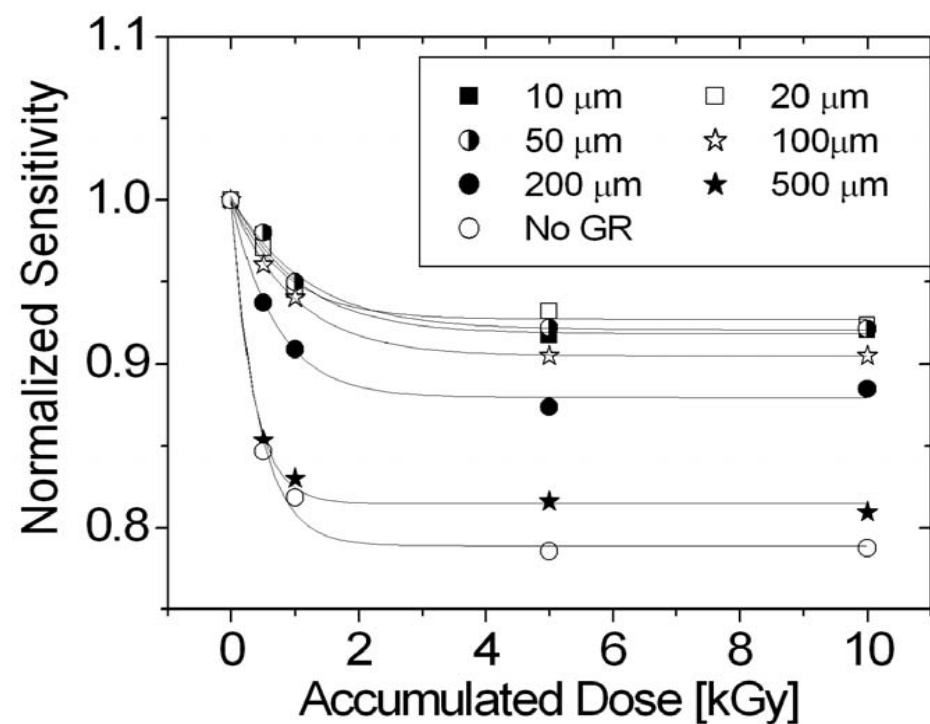
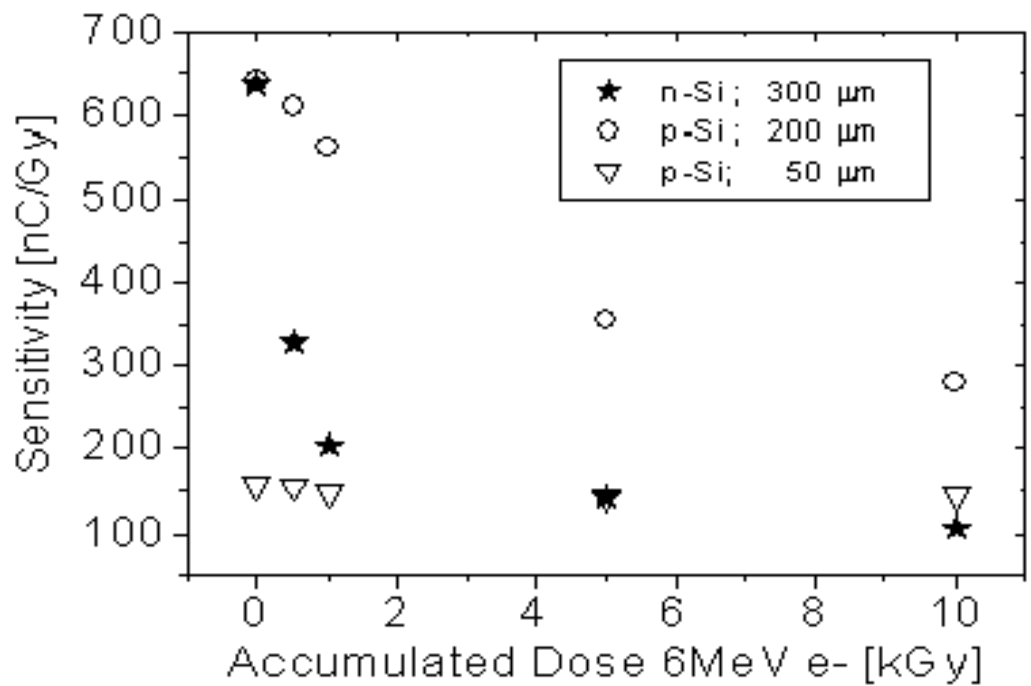
$$1/\tau - 1/\tau_0 = \sigma v_{th} N_t, \quad N_t = a \phi; \quad a = \text{trap generation rate}$$

σ capture cross section ; v_{th} carrier thermal velocity. N_t trap concentration.

$a_{DOFZ} < a_{SFZ} \Rightarrow$ increased radiation hardness of the device to radiotherapeutic beams.

$$a_{DOFZ} = 5.0 \times 10^7 \text{ cm}^{-3}\text{Gy}^{-1}, \quad a_{SFZ} = 8.1 \times 10^7 \text{ cm}^{-3}\text{Gy}^{-1}$$

Improved stability of the sensitivity with the accumulated dose by using epitaxial Si (p-type) with guard ring to confine the active volume of the device



M. Bruzzi et al. App. Phys. Lett, 2007.

Italian patent No. FI2006A000166

High-bandgap semiconductor detectors

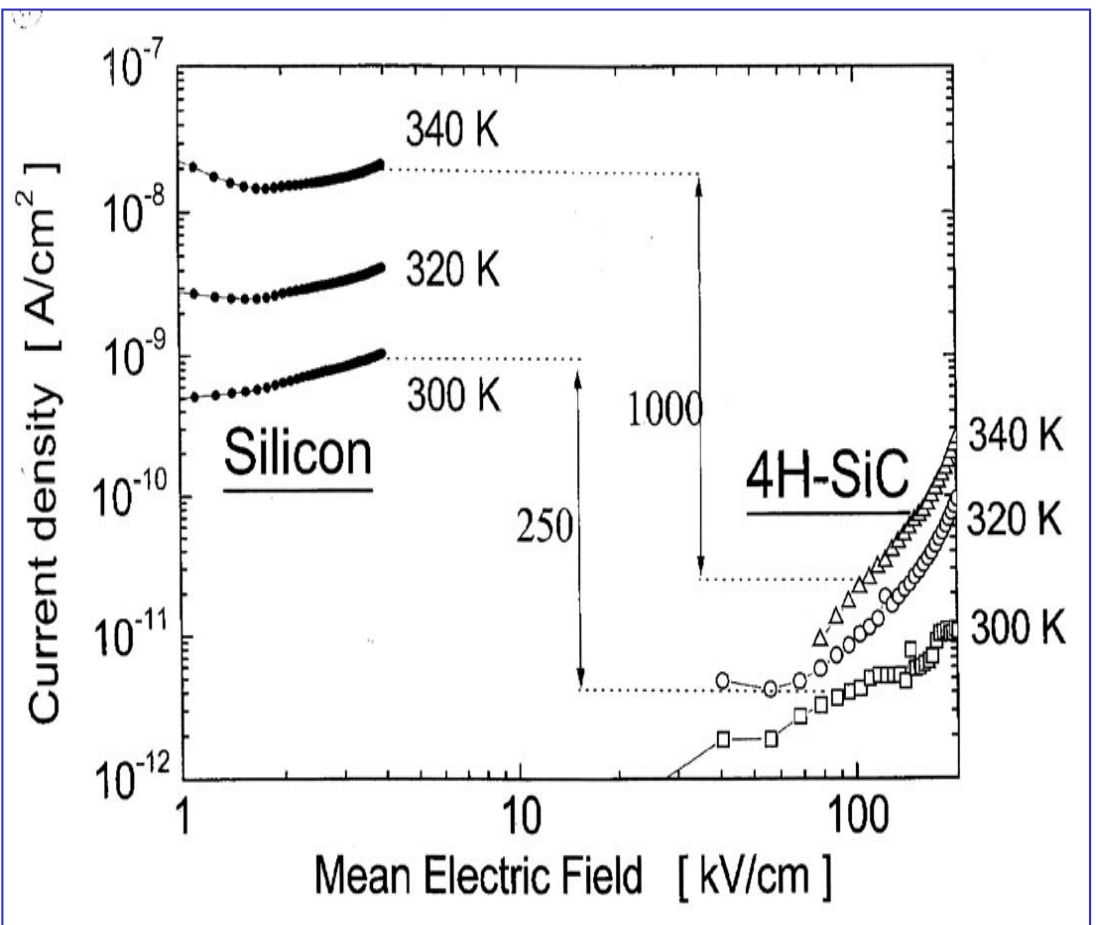
Property	Si	Diamond Polycrystal	Diamond single crystal	4H SiC
Material	MCz, FZ, epi	Polycrystal	single crystal	epitaxial
E _g [eV]	1.12	5.5	5.5	3.3
E _{breakdown} [V/cm]	3·10 ⁵	10 ⁷	10 ⁷	2.2·10 ⁶
μ _e [cm ² /Vs]	1450	1800	>1800	800
μ _h [cm ² /Vs]	450	1200	>1200	115
v _{sat} [cm/s]	0.8·10 ⁷	2.2·10 ⁷	2.2·10 ⁷	2·10 ⁷
Z	14	6	6	14/6
ε _r	11.9	5.7	5.7	9.7
e-h energy [eV]	3.6	13	13	7.6
Density [g/cm ³]	2.33	3.515	3.515	3.22
Displacem. [eV]	13-20	43	43	25
e-h/μm for mips	~80	36	36	55
Max ccd [μm]	>500	300	800	55
Max wafer φ	6"	6"	~1.4cm	2"
Commercial	yes	H.Kagan talk	H.Kagan talk	limited
CERN R&Ds	RD50, RD39	RD42	RD42	RD50

Main Advantage:

High band gap semiconductors show a stable or even decreased leakage current after irradiation: recombination increases and generation is not favoured at room T (it is dominated by emission from midgap centers).

La corrente di fuga varia di ordini di grandezza al variare del gap del materiale. Per SiC e diamante densità tipiche di corrente <1pA/cm², indipendentemente dalla fluenza di irraggiamento.

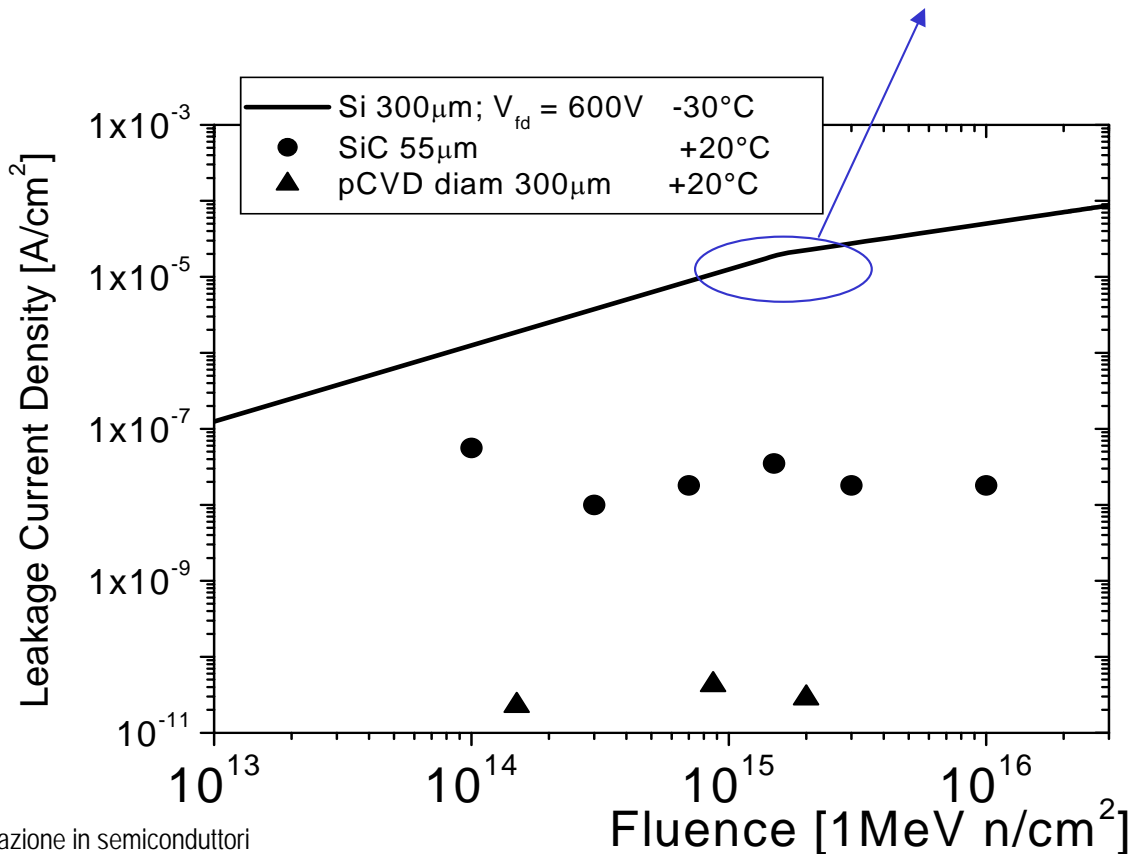
Silicon: $J(\Phi) = \alpha \cdot \Phi \cdot d$



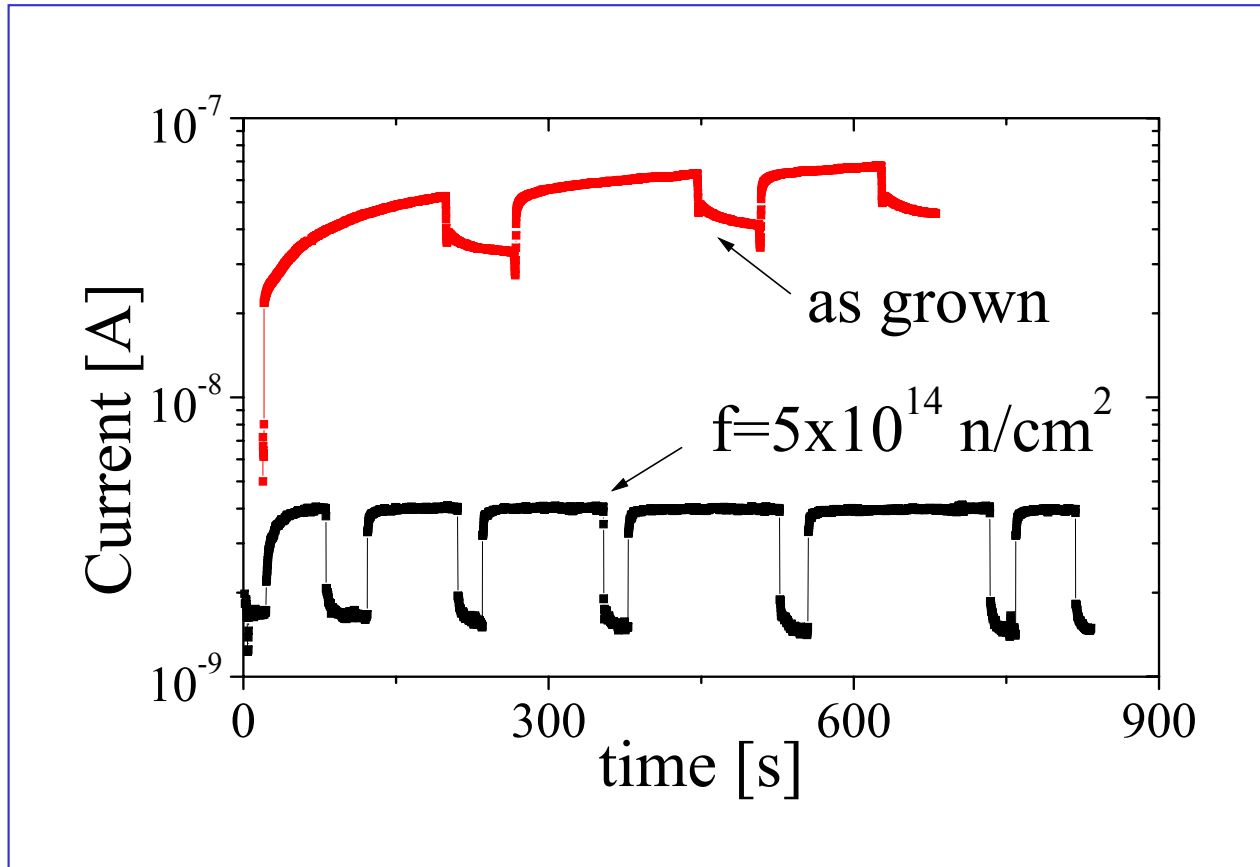
$T = -30^\circ\text{C}; V = 600\text{V}, W = 300\mu\text{m}$

$$I(T) \propto T^2 \exp\left(-\frac{E_g}{KT}\right)$$

Partial depletion



L'irraggiamento con elevate fluenze può anche migliorare le prestazioni del dispositivo: per esempio questo avviene nel dosimetro al diamante



Le proprieta' dosimetriche dopo irraggiamento con neutroni migliorano drasticamente a causa della rimozione di livelli energetici profondi

M. Bruzzi et al. App.Phys.Lett. (2002)

Forte diminuzione dei segnali TSC e PICTS relativi ai difetti responsabili della instabilità di corrente dopo irraggiamento con neutroni a tale fluenza

2

Appl. Phys. Lett., Vol. 81, No. 1, 1 July 2002

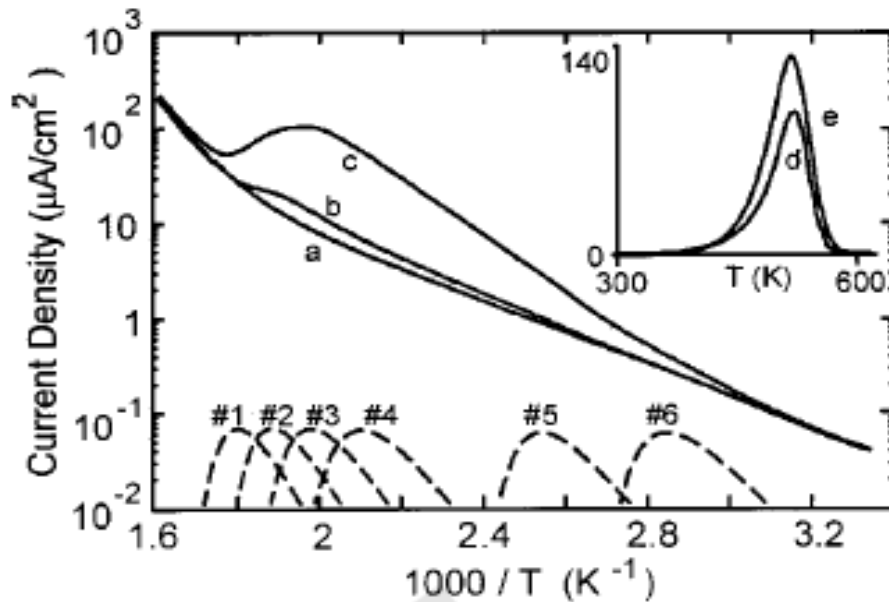


FIG. 1. TSC measurements performed with heating rate $\beta=0.15 \text{ K/s}$ and $V_{\text{bias}}=100 \text{ V}$. The background current (a) is measured without excitation. The other curves in the main plot correspond to measurements performed after a 30 min excitation using the Xe lamp, before (c) and after (b) NI. The contributions of fit components Nos. 1–6, calculated with arbitrary amplitudes, are shown in the bottom (dashed lines) for comparison. The spectra in the inset have been measured after a priming with a Co^{60} γ -source, up to a dose of 8 Gy; the signal measured after NI (d) is multiplied by ten for better comparison with the spectrum measured before NI (e).

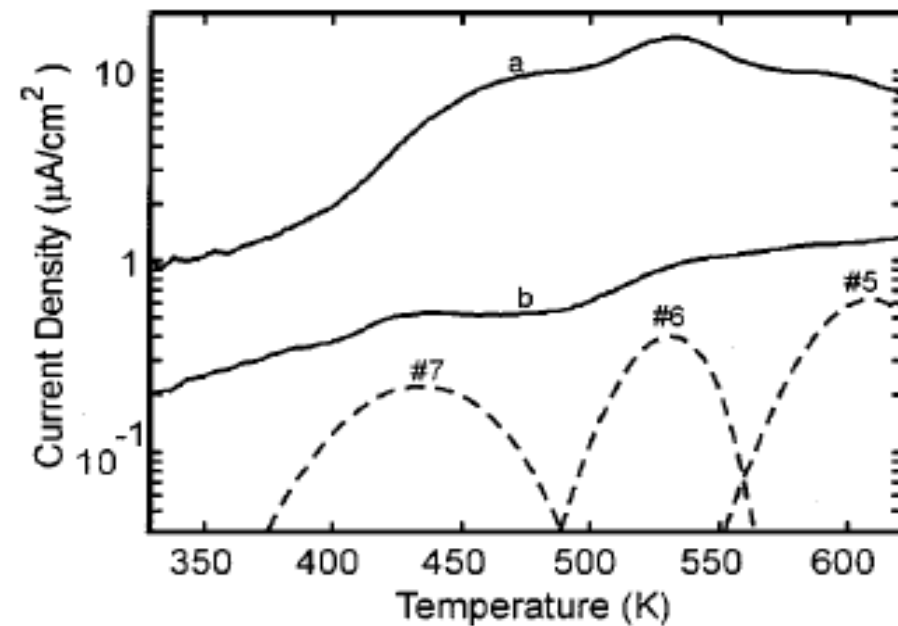
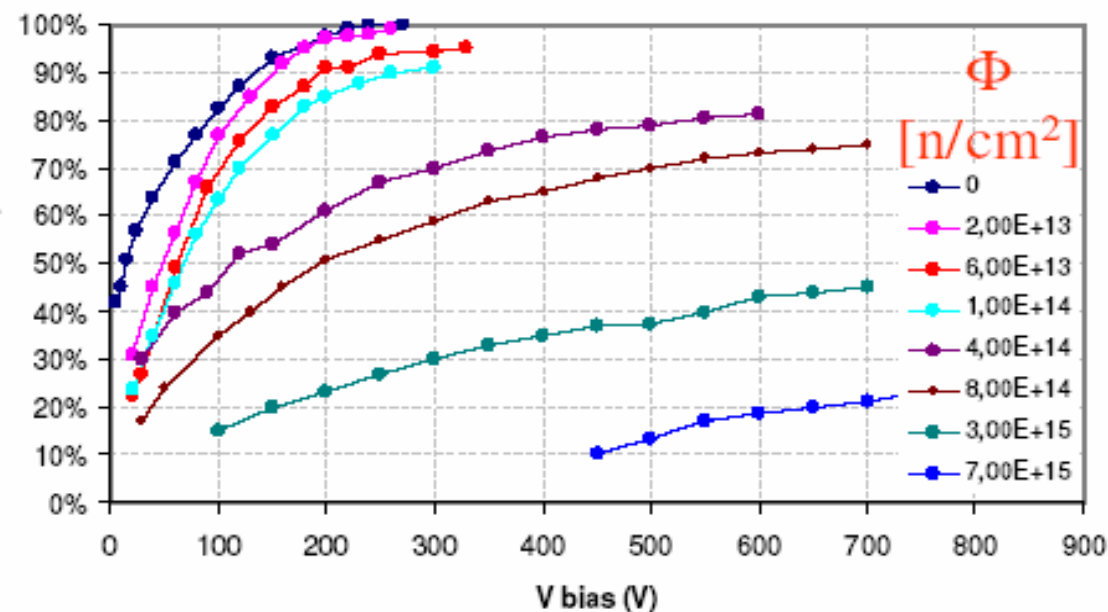


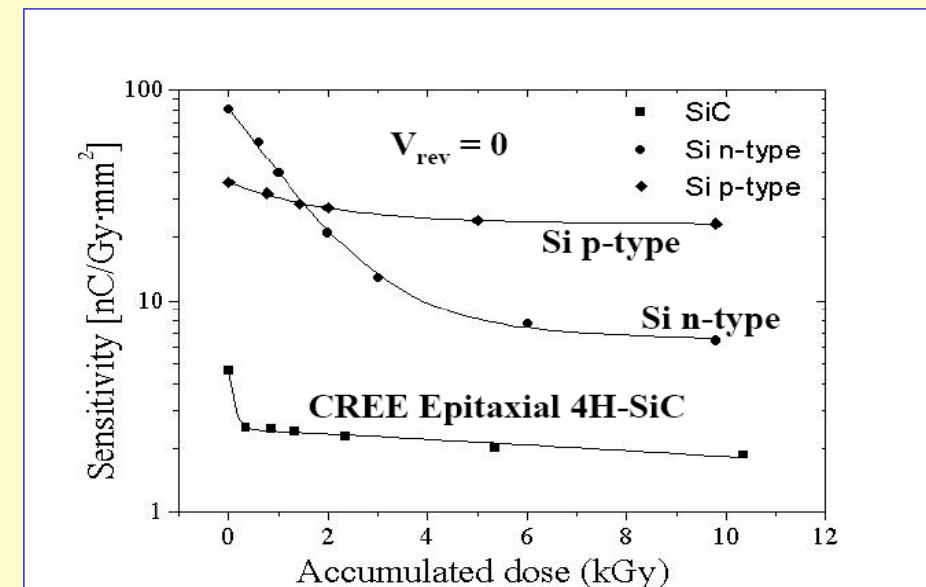
FIG. 2. PICTS spectra measured before (a) and after (b) NI. The calculated spectral lines corresponding to deep levels Nos. 5–7 are reported in the bottom (dashed lines), with arbitrary amplitude, for comparison.

SiC: not radiation resistant as a high energy physics detector and a radiotherapy dosimeter.



[F. Nava, INFN & University of Modena, Oct. 2004]

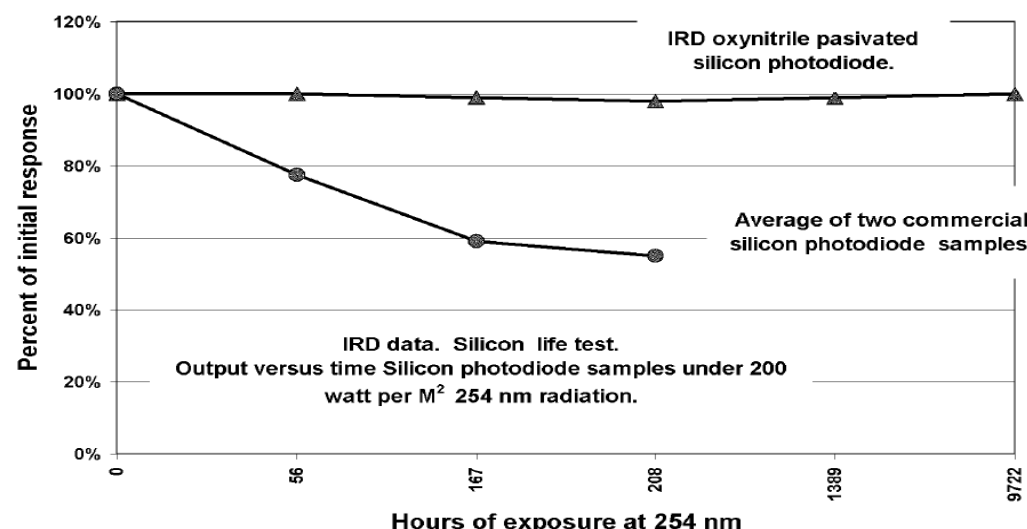
Sensitivity vs. Accumulated Dose after irradiation with Cs^{137}



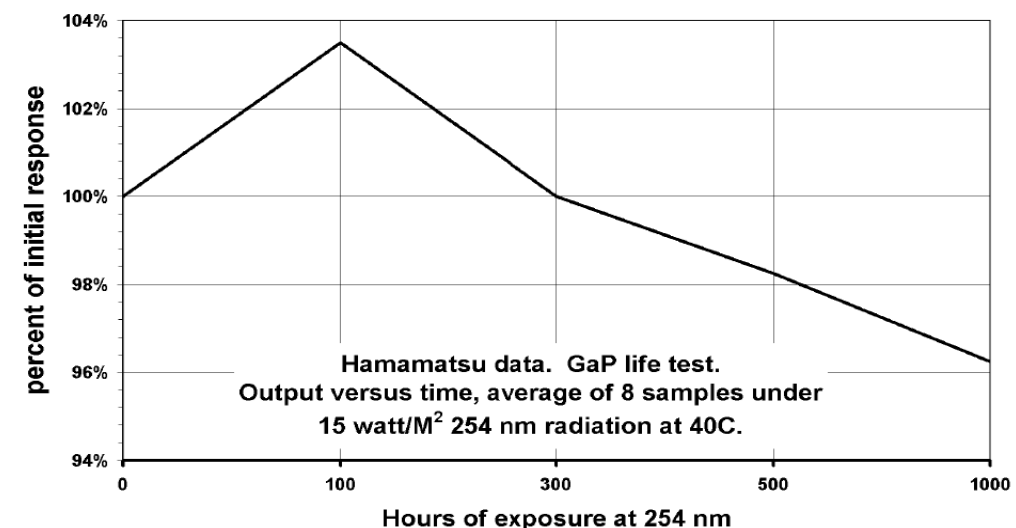
M. Bruzzi et al, RESMDD02, 2002

But good radiation resistance as UV photodetector, extremely stable for long periods of time even when exposed to high doses of UV radiation of up to 100W/m^2

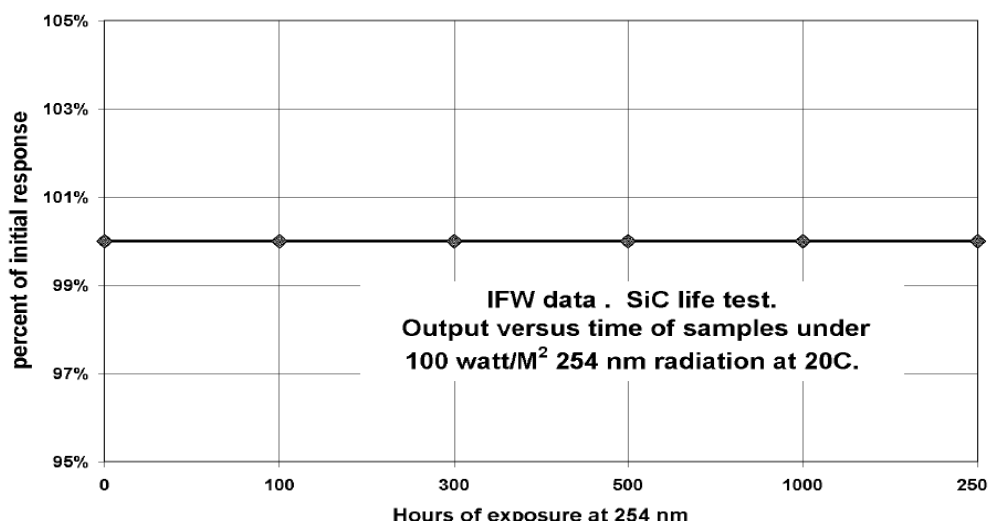
Silicon Output versus 254 nm dose



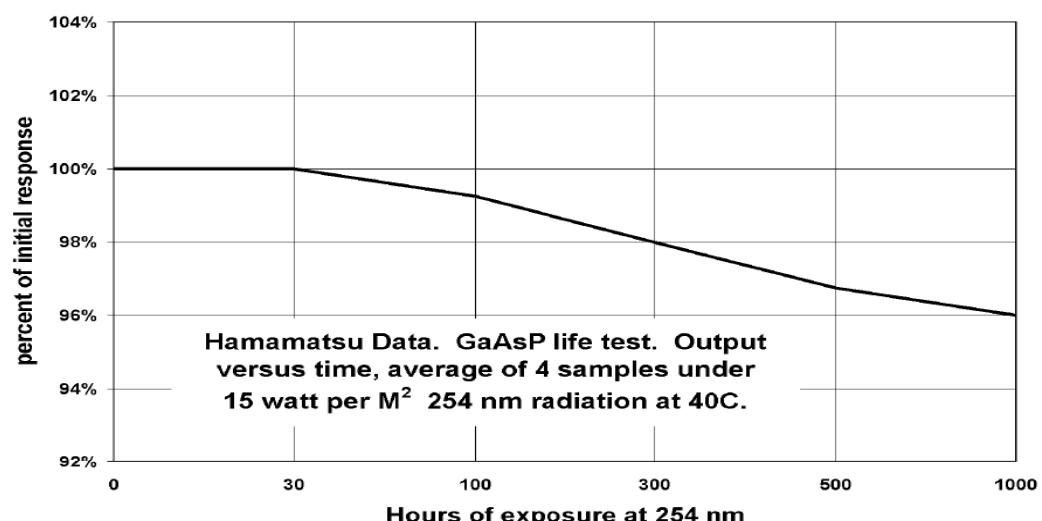
GaP variance in output versus 254 nm UV Dose



SiC variance in outout versus 254 nm dose



GaAsP variance in output versus 254 nm UV dose



Summary

- **Radiation damage of semiconductors can be understood in terms of microscopic disorder.**
- **Material engineering allowed to improve the radiation resistance of Si detectors for the development of tracking detectors for SLHC-experiments, under study by the CERN-RD50 collaboration.**
- **Material engineering concepts have proved to be useful also for other application fields (e.g. in dosimetry)**
- **Radiation can be beneficial: e.g. it cures instability of response in diamond dosimeters.**
- **High bandgap materials are intrinsically radiation hard in terms of leakage current.**